creative commons
COMMONS DEED

저작자표시-비영리-변경금지 2.0 대한민국

이용자는 아래의 조건을 따르는 경우에 한하여 자유롭게

- 이 저작물을 복제, 배포, 전송, 전시, 공연 및 방송할 수 있습니다.

다음과 같은 조건을 따라야 합니다:

저작자표시. 귀하는 원저작자를 표시하여야 합니다.

비영리. 귀하는 이 저작물을 영리 목적으로 이용할 수 없습니다.

변경금지. 귀하는 이 저작물을 개작, 변형 또는 가공할 수 없습니다.

- 귀하는, 이 저작물의 재이용이나 배포의 경우, 이 저작물에 적용된 이용허락조건을 명확하게 나타내어야 합니다.
- 저작권자로부터 별도의 허가를 받으면 이러한 조건들은 적용되지 않습니다.

저작권법에 따른 이용자의 권리는 위의 내용에 의하여 영향을 받지 않습니다.

이것은 이용허락규약(Legal Code)을 이해하기 쉽게 요약한 것입니다.

Disclaimer

dCollection

연세대학교
YONSEI UNIVERSITY

Physiologically Based Pharmacokinetic Modeling and Simulation of Thiazolidinediones in Patients with Hepatic Impairment

Jungsin Park

The Graduate School
Yonsei University
Department of Pharmaceutical Medicine
and Regulatory Science

연세대학교
YONSEI UNIVERSITY

Physiologically Based Pharmacokinetic Modeling and Simulation of Thiazolidiendiones in Patients with Hepatic Impairment

A Dissertation
Submitted to the Department of Pharmaceutical Medicine
and Regulatory Science
and the Graduate School of Yonsei University
in partial fulfillment of the
requirements for the degree of
Doctor of Philosophy

Jungsin Park

December 2021

연세대학교
YONSEI UNIVERSITY

This certifies that the dissertation of Jungsin Park is approved.

Supervisor: Min Soo Park

Min Jung Chang: Committee Member #1

Choon Ok Kim: Committee Member #2

Tae Gon Hong: Committee Member #3

Jung Il Lee: Committee Member #4

The Graduate School

Yonsei University

December 2021

연세대학교
YONSEI UNIVERSITY

ACKNOWLEDGEMENT

I would like to thank my supervisor Professor Min Soo Park and Professor Choon Ok Kim for their dedicated support and guidance. Without their enthusiasm, encouragement, and continuous optimism I would hardly a long and arduous process.

My deep and sincere gratitude to my father, Mr. Suk Yong Park, and to my mother, Mrs. Young Soon Kim, for their continuous and unparalleled love, help, and support. I am forever indebted to my parents for giving me the opportunities and experiences that have made me who I am. They selflessly encouraged me to explore new directions in life and seek my own destiny. This journey would not have been possible if not for them, and I dedicate this milestone to them.

연세대학교
YONSEI UNIVERSITY

Contents

연세대학교
YONSEI UNIVERSITY

연세대학교
YONSEI UNIVERSITY

List of Tables

연세대학교
YONSEI UNIVERSITY

연세대학교
YONSEI UNIVERSITY

List of Figures

연세대학교
YONSEI UNIVERSITY

연세대학교
YONSEI UNIVERSITY

Abstract

Physiologically Based Pharmacokinetic Modeling and Simulation of Thiazolidinediones in Patients with Hepatic Impairment

Jungsin Park

Department of Pharmaceutical Medicine and Regulatory Science

The Graduate School

Yonsei University

Background

The prevalence of liver disease in diabetic patients is very high. As the liver is the major organ responsible for glycemic control and drug elimination, pharmacokinetic (PK) evaluation of antidiabetic drugs is essential in patients with hepatic impairment.

연세대학교
YONSEI UNIVERSITY

Thiazolidinedione (TZD) drugs (e.g., lobeglitazone, rosiglitazone, and pioglitazone) — agonists of peroxisome proliferator-activated receptor−γ (PPAR−γ) —increase insulin sensitivity. TZDs share many PK characteristics. Lobeglitazone, rosiglitazone, and pioglitazone have high bioavailability (80—90%) with short times to reach peak concentration (T_{max} ~1h). These drugs are highly bound to serum albumin (>99%), are mainly metabolized by liver enzymes, and excreted as metabolites; the renal excretion of the parent drugs is negligible. Hepatic metabolism is the main route of elimination. Therefore, the PK parameters of TZDs can be significantly altered in patients with hepatic impairment, varying according to the severity of impairment. In principle, clinical trials should be conducted on patients with hepatic impairment to obtain the PK parameters for these drugs. However, there are many difficulties associated with such trials, especially with respect to recruiting patients and safety issues. Recently, PK modeling and simulation methods have been focused to overcome such limitations of clinical trials.

The physiologically based pharmacokinetic (PBPK) modeling and simulation approach combines chemical properties, biochemical reactions, and physiological characteristics to predict the absorption, distribution, and elimination of a drug after administration. This method can be used, instead of conducting clinical trials, to predict PK parameters in patients with various diseases, children, and pregnant women.

연세대학교
YONSEI UNIVERSITY

The purpose of this study was to develop PBPK models of lobeglitazone, rosiglitazone, and pioglitazone in patients with hepatic impairment of varying severity, as defined by the Child-Pugh classification system.

Method

The population-based software, SimCYP^{TM} version 18.1 (Certara, St. Louis, MO, USA) was used to develop PBPK models of lobeglitazone, rosiglitazone, and pioglitazone. The input parameters related to the physicochemical properties of these drugs were obtained from the open-source database, DrugBank (go.drugbank.com). The required *in vitro* experimental values were obtained by searching the literature. The patient demographics of hepatic impairment were defined based on previous reports of different phenotypes of hepatic enzymes and varying degrees of pathophysiology.

To develop PBPK models, a first-order kinetic absorption model was applied for lobeglitazone and rosiglitazone, whereas an advanced dissolution, absorption, and metabolism (ADAM) model was applied for pioglitazone. The full-body distribution model was applied to represent each major organ as a compartment connected by blood flow. Based on *in vitro* information about relevant hepatic enzymes, the enzyme kinetic model was selected for all TZDs to analyze different contributions of the intrinsic clearance of each enzyme to decreased liver function, with the

연세대학교
YONSEI UNIVERSITY

severity of the hepatic impairment stratified according to the Child-Pugh classification system.

The developed PBPK models were validated with the major PK parameter values (especially for the peak concentrations, $C_{max,}$ and the areas under the concentration–time curve, AUCs) from simulation results obtained for virtual populations and compared to those from clinical trials in age- and sex-matched healthy subjects. The acceptable range for the predicted capability of the models was from 0.5 to 2.0 for the ratios of the predicted and observed PK parameters. For lobeglitazone, an additional evaluation of the model was accomplished by comparing the simulated PK parameters to the values from the available clinical trials in Child-Pugh A and B patients to determine whether the model was applicable to patients with hepatic impairment.

The validated PBPK models of the TZDs were simulated in 100 virtual, healthy, Child-Pugh A, B, or C subjects cases aged 18–65 years, with a 50:50 male:female ratio. The major PK parameters of the simulation results were subsequently compared among all groups (healthy population, Child-Pugh A, B, and C).

Results

The developed PBPK models of lobeglitazone, rosiglitazone, and pioglitazone in this study were valid, with the ratio of each predicted major PK parameter value of simulations to the observed value of clinical trials within the acceptable range for

연세대학교
YONSEI UNIVERSITY

healthy subjects. The prediction errors (PEs) of C_{max} and AUC were 0.84 and 0.97 for lobeglitazone; 0.86 and 0.88 for rosiglitazone; and 0.94 and 0.91 for pioglitazone, respectively. There were no significant differences between the predicted PK values and the observed values for lobeglitazone in Child-Pugh A and B patients. Hence, the validity of the model was additionally confirmed: the PEs of C_{max} and AUC were 0.94 and 1.49 in Child-Pugh A patients and 1.10 and 1.20 in Child-Pugh B patients.

The simulation results showed that the major PK parameters of all TZDs in the Child-Pugh A patients were not significantly different from those in healthy populations; the geometric mean ratios (GMRs) were between 0.5 and 2.0 for C_{max} and AUC. In Child-Pugh B patients, the GMRs for AUC and C_{max} were 1.36 and 0.97 for lobeglitazone, 1.93 and 0.92 for rosiglitazone, 2.19 and 1.03for pioglitazone, respectively. The GMRs of AUC and C_{max} were 1.94 and 0.92 for lobeglitazone, 2.26 and 0.81 for rosiglitazone, and 2.76 and 0.91 for pioglitazone, respectively, in Child-Pugh C patients. Additional analysis also revealed a significant alteration in the unbound fraction (f_u) based on the severity of hepatic impairment. The GMRs of AUC for f_u of lobeglitazone were as follows: 1.51, 2.50, and 3.62 for lobeglitazone; 1.73, 3.23, and 5.66 for rosiglitazone; 1.78, 2.82, and 4.56 for pioglitazone in Child-Pugh A, B, and C patients, respectively.

Discussion

연세대학교
YONSEI UNIVERSITY

The current PBPK models of TZDs, applied as full-body distribution model considering the functional liver volume, hepatic enzyme activities, blood flow, and serum proteins could be used to predict PK alterations in patients with hepatic impairment, grouped according to the Child-Pugh classification system.

Compared to the previous report, the simulation results of the lobeglitazone PBPK model were inconsistent with the observed values in healthy subjects, and Child-Pugh A and B patients. Thus, the simulation results in Child-Pugh C patients could be used for reference, although the model tended to slightly overpredict the AUC in patients with hepatic impairment. The simulation of the rosiglitazone model showed increased AUCs, consistent with previous reports in patients with hepatic impairment. However, the simulation of the pioglitazone model overpredicted AUCs in patients with hepatic impairment. This could be due to the nature of PBPK modeling to overpredict AUCs in hepatic impairment, not taking the transporter activity into account in this model, or not considering CYP2C8 genetic polymorphisms in the observed data used for the validation of the model.

Nonetheless, the PBPK model and simulation in this study were noteworthy because the results provided evidence supporting the results of clinical trials. The PK parameters could be compared among healthy subjects and patients with Child-Pugh A, B, and C based on the simulation results. In addition, the PBPK models enabled the evaluation of the unbound fraction in healthy subjects and patients with

연세대학교
YONSEI UNIVERSITY

hepatic impairment by severity, which was not feasible due to technical limitations to measure these values in the clinical trials.

Conclusion

The predictive capability of PBPK modeling and simulation in this study would be appropriate and could be applied to prediction of PK parameters of TZDs in patients with hepatic impairment graded according to the Child-Pugh classification system. Thus, the PBPK modeling and simulation could be notable to give supplementary information under those limited condition to conduct of clinical trials in specific patient groups.

KEYWORDS: Lobeglitazone, Rosiglitazone, Pioglitazone, Hepatic impairments, Physiological based pharmacokinetics modeling and simulation

연세대학교
YONSEI UNIVERSITY

1. Introduction

1.1. Background

The global prevalence of adult diabetes was 8.8% in 2015 and is predicted to rise to ~10.4% in 2040, with type 2 diabetes mellitus accounting for more than 90% of all diabetes cases (Ogurtsova et al. 2017). Patients with diabetes have a high prevalence of various liver diseases, including nonalcoholic fatty liver disease, cirrhosis, and acute liver failure (Tolman et al. 2007). In patients with hepatic impairment, the pharmacokinetic (PK) profiles of drugs can be affected due to reduced activity of hepatic enzymes, reduced synthesis of plasma proteins (e.g., serum albumin), and changing hepatic blood flow (Rodighiero 1999). Therefore, it is essential to perform PK studies of antidiabetic drugs in patients with hepatic impairment.

Thiazolidinediones (TZDs) are a class of insulin sensitizers. They are agonists of the transcription factor, peroxisome proliferator-activated receptor-γ (PPAR-γ), and modulates glucose homeostasis (Cariou, Charbonnel, Staels 2012). Despite the benefit of glycemic control, the European Medicines Agency withdrew rosiglitazone (Avandia®) and pioglitazone (Actos®); the Food and Drug Administration withdrew rosiglitazone due to a risk of heart attack (Soccio, Chen, Lazar 2014). However,

연세대학교
YONSEI UNIVERSITY

lobeglitazone (Duvie®), rosiglitazone, and pioglitazone are marketed in Korea. Thus, TZDs should be used with special cautions.

TZDs have a common pharmacological mode of action. Moreover, they share some PK properties despite differences in their hepatic metabolism (Table 1). Orally administered TZDs are absorbed rapidly (time to the peak concentration (T_{max})<2 h) with high bioavailability (≥ 80%). They all have a relatively small volume of distribution (≤0.3 L/kg) and low hepatic extraction with high albumin binding (≥ 99%). TZDs are extensively metabolized in the liver and are excreted as metabolites mostly through the bile or feces; renal elimination is negligible. Thus, hepatic impairment in patients using TZDs may lead to significant PK alterations that might cause subsequent clinical consequences.

A clinical PK study has been conducted for lobeglitazone in patients with hepatic impairments of Child-Pugh A and B classes with matched controls (n=6 per group). Two studies have reported changes in the PK parameters of rosiglitazone and pioglitazone in patients with hepatic impairment (n=18 for rosiglitazone, n=12 for pioglitazone) (Eckland, Danhof 2000, Miller et al. 1999). Although these studies showed PK alterations of each TZD in patients with hepatic impairment, they did not provide any information about PK changes due to the severity of hepatic impairment or about unbound fraction measurements. In principle, additional clinical trials should be conducted on patients with hepatic impairment to obtain

연세대학교
YONSEI UNIVERSITY

accurate PK data. However, in reality, it is difficult to conduct any clinical trial due to safety issues and difficulties in patient recruitment. Modeling and simulation methods have been widely applied to overcome these real-world difficulties in conducting clinical research on patients with various disease (El-Khateeb et al. 2021).

Physiologically based pharmacokinetic (PBPK) modeling and simulation is an approach that incorporates not only the drug properties but also biochemical reactions and physiology of human beings to predict PK parameters of those drug (Zhuang, Lu 2016). In addition, it is possible to predict the effects of various patient characteristics, such as age, height, weight, serum protein levels, and disease states, on the absorption, distribution, metabolism, and excretion (ADME) of drugs. Focusing on the mechanistic approach based on the mathematical description extending from the molecular level to the whole body, these complexities of the relationship between intrinsic and extrinsic factors and PK parameters of drugs can be partially solved to predict concentration–time curves after the administration of the drugs in children, the elderly, pregnant women, and patients with various diseases (Tyluki, Polak, Winśniowska 2016). Prediction methods in special populations with PBPK modeling and simulation are currently expected fields in terms of drug discovery and development as well as regulation (Zhao et al. 2011)

The physiological characteristics of patients with hepatic impairment have well described based on the severity of the disease and common PK alterations have been

연세대학교
YONSEI UNIVERSITY

quite well described (Delcò et al. 2005, Verbeeck 2008). Using previously reported population-specific information related to PK in patients with hepatic impairment and drug-specific physicochemical data, a mechanistic approach to evaluate PK changes of various drugs can be extended from the molecular level to the physiological level. Statistical population PK parameters can be predicted based on the distribution of population in ages and the Monte Carlo method.

연세대학교
YONSEI UNIVERSITY

Table 1. Comparison of thiazolidinediones

	Lobeglitazone	Rosiglitazone	Pioglitazone
References	(Bae et al. 2021)	(Malinowski, Bolesta 2000)	(Hanefeld 2001)
Chemical structures	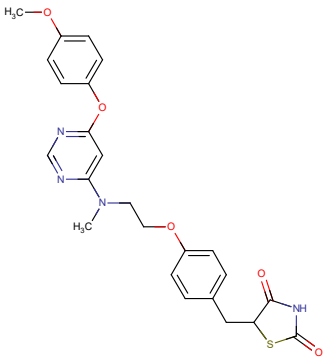	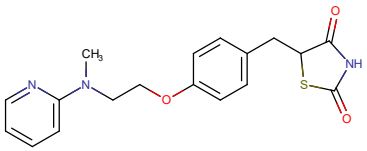	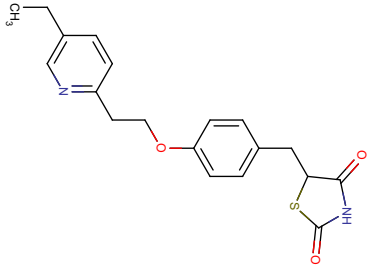
Dosages	0.5 mg PO once daily	4 mg PO once or twice daily	15 mg PO once daily
Protein bindings (Major binding protein)	>99% (Albumin)	>99% (Albumin)	>99% (Albumin)
T_{max} (h)	1	1.75	2
F_{oral}	>90%	>90%	>80%

연세대학교
YONSEI UNIVERSITY

Hepatic extraction ratio	Low	Low	Low
V_d (L/kg)	0.19–0.28 L/kg	0.21 L/kg	0.25 L/kg
Metabolism	In the liver	In the liver	In the liver
Hepatic enzymes	CYP2C19 CYP2D6 CYP3A4	CYP2C8 CYP2C9	CYP2C8 CYP3A4

Abbreviation: PO, per os; T_{max}, time to peak concentration; F_{oral}, oral bioavailability; V_d, the volume of distribution; $t_{1/2}$, half-life; CYP, cytochrome P450.

연세대학교
YONSEI UNIVERSITY

1.2. Purpose of the Study

The main objectives of this study were to develop PBPK models of marketed TZDs (lobeglitazone, rosiglitazone, and pioglitazone) in healthy subjects and patients with hepatic impairment, verify the PBPK models based on currently available clinical results, and apply the models to predict PK parameters in patients with hepatic impairment graded according to the Child-Pugh classification system.

연세대학교
YONSEI UNIVERSITY

2. Method

2.1. PBPK Modeling Platform and Strategy

The population-based PBPK simulator SimCYP™ version 18 release 2 (Certara, St. Louis, MO, USA) was used in this study. SimCYP™ is a platform for mechanistic modeling and simulation of the process of ADME of drugs in healthy and diseased populations (Jamei et al. 2009, Zhuang, Lu 2016). The SimCYP™ simulator interplays demographic, genetic, anatomical, physiological, and drug-specific factors to predict PK properties (Figure 1). The platform contains a validated, population-specific physiological database. The physicochemical properties of drugs can be used to predict the interplays of compounds with biological molecules or proteins at the cellular level (Jónsdóttir, Jørgensen, Brunak 2005). By considering the composition of tissues and organ volumes, the interactions of molecules can be expended to the organ levels, and the complete PK profiles of drugs can be estimated by the connecting each organ with blood flow in the body and combining all information about population, drug-specific, and PK processes.

연세대학교
YONSEI UNIVERSITY

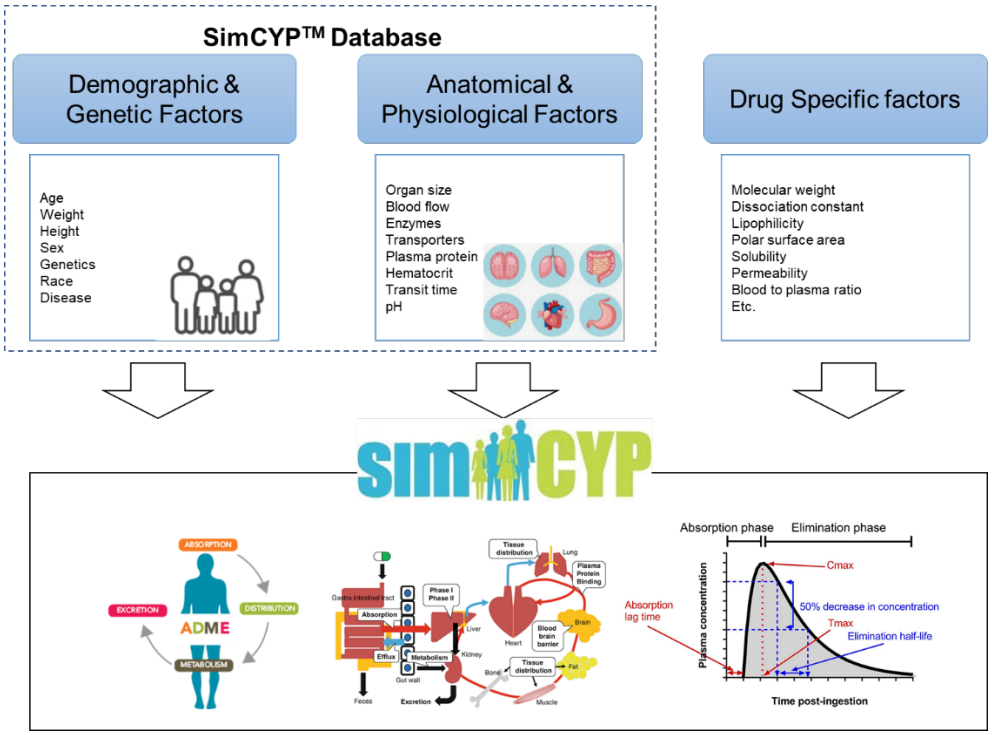

Figure 1. The overview of SimCYP™ simulator.

The principal elements implemented and required data in the simulator. Modified from (Jamei et al. 2009).

연세대학교
YONSEI UNIVERSITY

The overall strategy of this study is illustrated in Figure 2. The representative clinical data were obtained by searching the literature. Then, the models of lobeglitazone, rosiglitazone, and pioglitazone were developed in virtual healthy subjects and verified by comparing the simulation data to observed data. These validated models were used to predict PK parameters in patients with hepatic impairment graded according to the Child-Pugh classification system, using population data included in the simulator.

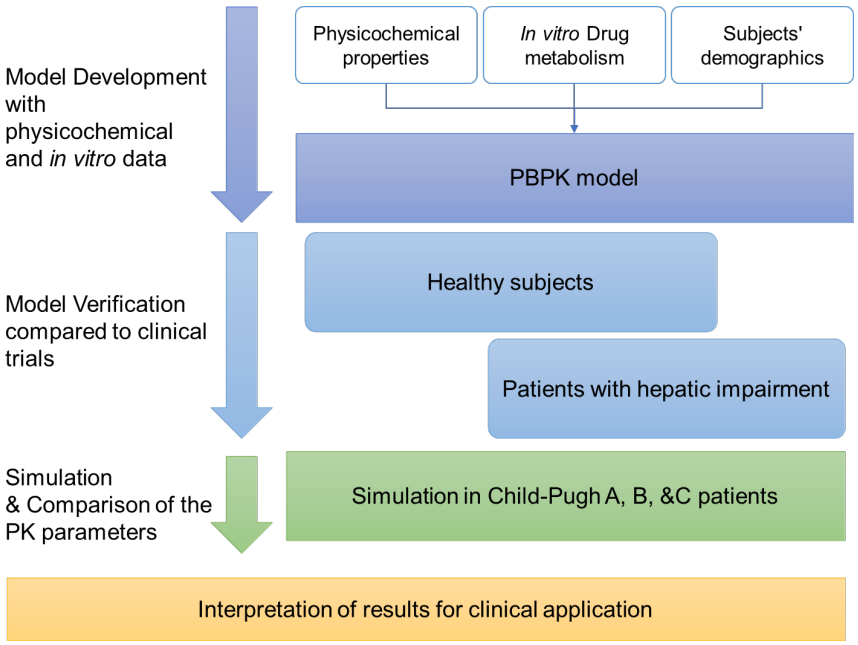

Figure 2. Overall strategy of the study.

PBPK model, physiologically based pharmacokinetic model; PK, pharmacokinetics.

연세대학교
YONSEI UNIVERSITY

2.1.1. Introduction of Virtual Populations

Physiological changes affecting the absorption, distribution, and elimination of drugs were taken into account in the calculations of PK parameters, especially with respect to age, sex, and various disease states (Figure 3). Age was linked to the body surface area; further, these baseline characteristics were related to blood flow and organ size. Virtual individuals were randomly selected using the Monte Carlo statistical sampling method in each trial, with the age range distributed according to the Weibull equation:

$$f(x) = \frac{\alpha}{\beta}\left(\frac{x}{\beta}\right)^{\alpha-1} e^{-(x/\beta)^{\alpha}} \quad (1)$$

Where, α and β were the parameters that define the distribution shape; *x* was the age and *f(x)* was the frequency of the number of subjects at age *x*. The age distribution was estimated by defining α and β as 2.1 and 24.7 for males; 1.9 and 24.7 for females, respectively.

Bodyweight and height were correlated to the factor of age, accordingly with coefficients of 2.643 and 175.32 and variability of 15% and 3.9% for males; 2.738 and 161.66 and variability of 18.8% and 3.9% for females, respectively.

연세대학교
YONSEI UNIVERSITY

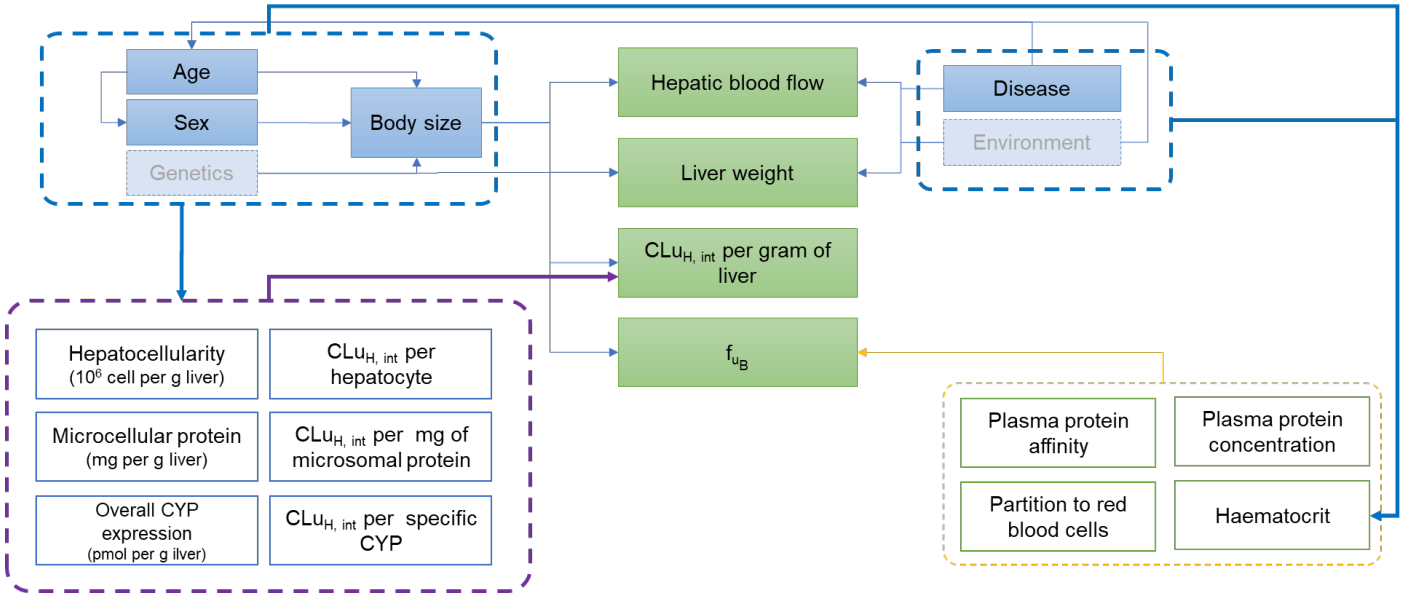

Figure 3. Influence of the characteristics of patients with hepatic impairment on PK of drugs.

Adapted from (Rostami-Hodjegan, Tucker 2007).

$CLu_{H,\,int}$, intrinsic clearance by hepatic enzymes; CYP, cytochrome P450; fu_B, unbound fraction.

연세대학교
YONSEI UNIVERSITY

2.2. PBPK Models in Healthy Subjects

2.2.1. Development of PBPK Models

The parameters used in PBPK modeling of TZDs (lobeglitazone, rosiglitazone, pioglitazone) are shown in Table 2. The physicochemical properties of molecules, including molecular weight, lipophilicity, compound type, and dissociation constants, were obtained from an official online database, DrugBank (Wishart et al. 2018). The unbound fraction values of rosiglitazone and pioglitazone were referred to the previous studies. The blood-to-plasma ratios of rosiglitazone and pioglitazone were 0.57 and 1, respectively (Tan et al. 2019). As the exact values of the unbound fraction (f_u^{human}) and blood-to-plasma ratio (B/P_{human}) of lobeglitazone in humans were unknown, the values were estimated using Eq (1) (Uchimura et al. 2010):

$$B/P_{human} = \frac{C_{Blood}}{C_{Plasma}} = \left(K_b \cdot f_u^{human} - 1\right) \times Ht_{human} + 1 \quad (1)$$

K_b is determined using Eq (2).

$$K_b = \frac{C_{rbc}}{C_{p,u}} = \frac{B/P_{rat} + Ht_{rat} - 1}{Ht_{rat}} \quad (2)$$

Where K_b is the ratio of the drug concentration in red blood cells (C_{rbc}) to the drug concentration of the unbound fraction in plasma (C_{pu}).

연세대학교
YONSEI UNIVERSITY

The murine unbound fraction (f_u^{rat}) and blood-to-plasma ratio (B/P_{rat}) of lobeglitazone were 0.00267 and 0.696, respectively (Yim et al. 2017). Both Ht_{rat} (ratio of hematocrit in rat) and Ht_{human} (ratio of hematocrit in human) were reported to be 0.45. The f_u^{human} and B/P_{human} of lobeglitazone were estimated to be 0.0001 and 0.55.

연세대학교
YONSEI UNIVERSITY

Table 2. Parameters of TZDs in PBPK modeling

Parameters (Unit)	Values		
	Lobeglitazone	**Rosiglitazone**	**Pioglitazone**
Molecular weight (g/mol)	480.5	357.4	356.4
Log*P*	4.3	2.9	3.8
Compound type	Zwitterions	Zwitterions	Monoprotic base
pK_a (acid)	7.61	7.64	6.66
pK_a (base)	3.96	6.43	
Fraction unbound	1.00×10^{-4}*	3.70×10^{-4}	2.07×10^{-3}
Blood-to-plasma ratio	0.55*	0.57	1
Absorption mode	First-order kinetics	First-order kinetics	ADAM Model
P_{eff},man (10^{-4} cm/s)	5.92†	6.52	2.66
MDCK II (10^{-6} cm/s)		34.3	
Polar Surface Area (Å^2)	102.88	71.53	68.29

연세대학교
YONSEI UNIVERSITY

Hydrogen Bond Donor (HBD)	1	1	1
Distribution	Full-body PBPK Model		
K*p* Scalar	1	1	0.33†
V_{ss} (L/kg)	0.149*	0.162*	0.213*
$P_{t:p}$ (Adipose)	0.173	0.159	0.365
$P_{t:p}$ (Bone)	0.191	0.220	0.069
$P_{t:p}$ (Brain)	0.020*	0.160	0.303*
$P_{t:p}$ (Gut)	0.223	0.245	0.132
$P_{t:p}$ (Heart)	0.177	0.185	0.116
$P_{t:p}$ (Kidney)	0.161	0.173	0.111
$P_{t:p}$ (Liver)	0.138	0.156	0.136
$P_{t:p}$ (Lung)	0.218	0.222	0.103
$P_{t:p}$ (Pancreas)	0.114	0.132	0.072
$P_{t:p}$ (Muscle)	0.066	0.078	0.048

연세대학교
YONSEI UNIVERSITY

$P_{t:p}$ (Skin)	0.315	0.328	0.142
$P_{t:p}$ (Spleen)	0.129	0.145	0.113
Elimination		Enzyme Kinetics	
Active Hepatic Scalar	7†	1	4†
rhCYP2C19 (μL/min/pmol)	11.6*	169.6	-
rhCYP2D6 (μL/min/pmol)	18.7*	84.6	-
rhCYP3A4 (μL/min/pmol)	33.4*	-	0.24*
rhCYP2C8 (μL/min/pmol)	-	-	2.38*
Additional Clearance HLM (μL/min/mg)	191.3*	35.7	5.80*

Abbreviation: logP, partition coefficient; pKa, acid dissociation constant; P_{eff}, man, regional in vivo huma intestinal effective permeability; MDCK II, Madin-Darby Canine Kidney strain II cells; Kp, tissue-to-plasma partition coefficient scalar; $P_{t:p}$, tissue-to-partition coefficients of specific organs calculated by Rodgers & Rowland theory or expand Rodger s &Rowland theory.* denotes the calculated data according to the explanation in the text. † denotes the optimized values compared to the reported values.

연세대학교
YONSEI UNIVERSITY

The absorption processes of orally administered TZDs via the gastrointestinal (GI) tract could be complicated by dynamic physiological changes through the GI tract, biochemical interactions with gut cells, and the physicochemical properties of drugs. There were 4 different models to be applicable in SimCYP^{TM}: the first-order kinetic absorption model; the compartmental absorption and transit model; the advanced dissolution, absorption, and metabolism (ADAM) model; and the multi-layer gut wall within the ADAM model. Each model was applied for lobeglitazone, rosiglitazone, and pioglitazone before selecting the final model by comparing the simulation results to the reported values. The first-order kinetic absorption was selected for lobeglitazone and rosiglitazone. This model assumed the GI tract to be a single cylindrical compartment (Figure 4). The effective gut wall permeability of the drug (P_{eff}, 10^{-4} cm/s) could be determined using the absorbed concentration ratio across the gut wall and the perfusion flow rate per area of the gut wall (Lennernäs 2014) (Eq (3)).

$$P_{eff} = \frac{C_{in} - C_{out}}{C_{out}} \cdot \frac{Q_{in}}{2\pi Rl} \quad (3)$$

Where, C_{in} and C_{out} are the inlet and outlet drug concentrations; R and l are the intestinal radius and length, respectively.

For lobeglitazone, P_{eff} was initially estimated to be 1.44 based on the apparent permeability, P_{aff} (7.39×10^{-6} cm/s) in the parallel artificial membrane permeability

연세대학교
YONSEI UNIVERSITY

assay (PAMPA) (Lee et al. 2015). However, the P_{eff} obtained from the experimental values could not predict the major PK parameters of lobeglitazone compared to the reported values, especially for T_{max} (delayed by more than 2 h compared to the reported values) and C_{max} (lower than 60% compared to the reported values) (Bae et al. 2021). Hence, the P_{eff} was optimized at 5.92 by repeat trials and modifications using the sensitivity analysis method implanted in SimCYP^{TM}.

For rosiglitazone, P_{eff} was calculated based on P_{aff} from an *in vitro* permeability assay and determined to be 34.3×10^{-6} cm/s in a Madin-Kidney Canine (MDCK) II cell-based assay (Varma et al. 2012).

$$P_{eff} = 10^{(Slope \times \log_{10} P_{aff}) + intercept} \quad (4)$$

For the P_{aff} in the MDCK II cell-based assay, the slope was determined to be 1.0117, and the intercept was -0.912 (Di et al. 2011).

As the physicochemical properties of pioglitazone were different from those of lobeglitazone and rosiglitazone (a monoprotic base), it was assumed that the dynamic pH changes throughout the GI tract might affect the permeability of the drug. Thus, the advanced dissolution, absorption, and metabolism (ADAM) model was applied for the absorption of pioglitazone. The ADAM model consisted of seven segments of the GI tract with slightly different regional pH values along the GI tract (Figure 4). The P_{eff} of pioglitazone was calculated using Eq (5) by taking into account

연세대학교
YONSEI UNIVERSITY

its physicochemical properties, such as polar surface area (*PSA*) and the number of hydrogen bond donors (*HBDs*) (Winiwarter et al. 1998):

$$\log P_{eff} = 4 - 2.546 - 0.011 \times PSA - 0.278 \times HBD \quad (5)$$

연세대학교
YONSEI UNIVERSITY

(a)

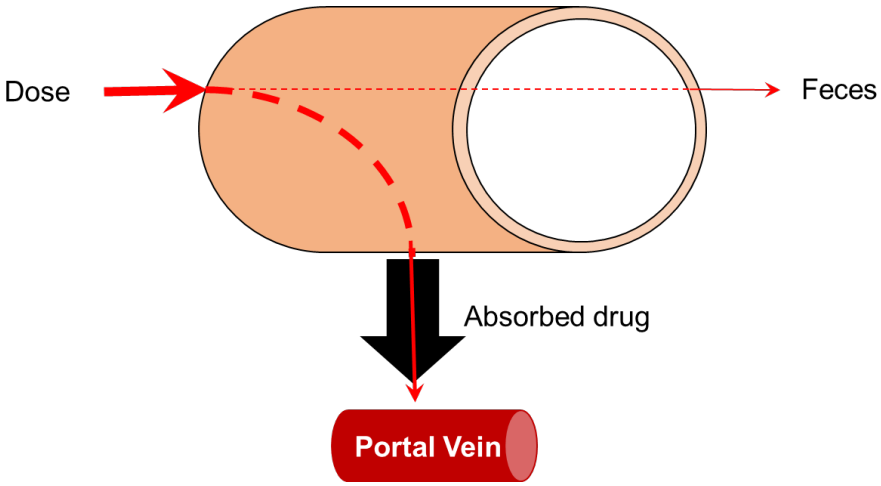

(b)

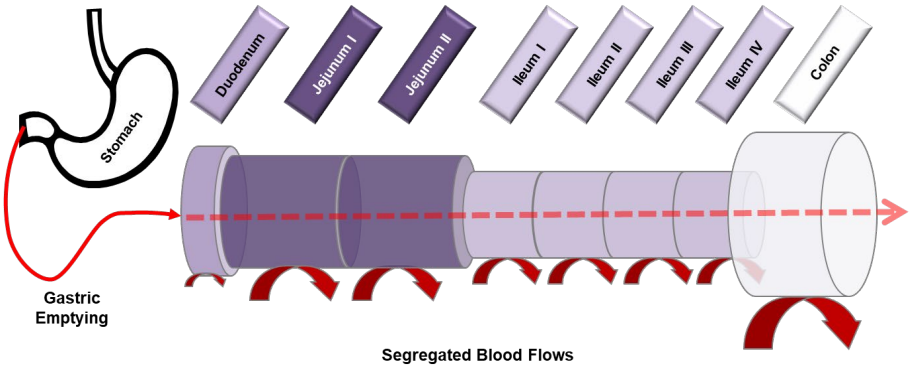

Figure 4. Schematic diagrams of the absorption models. (a) a first-order kinetic model applied for lobeglitazone and rosiglitazone. (b) an advanced dissolution, absorption, and metabolism (ADAM) model applied for pioglitazone.

Red lines indicate the route of the dissolved drug. Modified from (Pathak et al. 2017).

연세대학교
YONSEI UNIVERSITY

The full-body PBPK distribution model was applied for all TZDs in this study to investigate the effects of the severity of hepatic impairment on functional liver portion and decreased enzymatic activity. The model was composed of 11 organs connected by blood circulation (Figure 5). Each compartment was defined by a tissue volume (V_{organs}) and blood flow rate (Q_{orans}), and these values were specific to sex, age, and disease states and based on the Weibull distribution (Table 3).

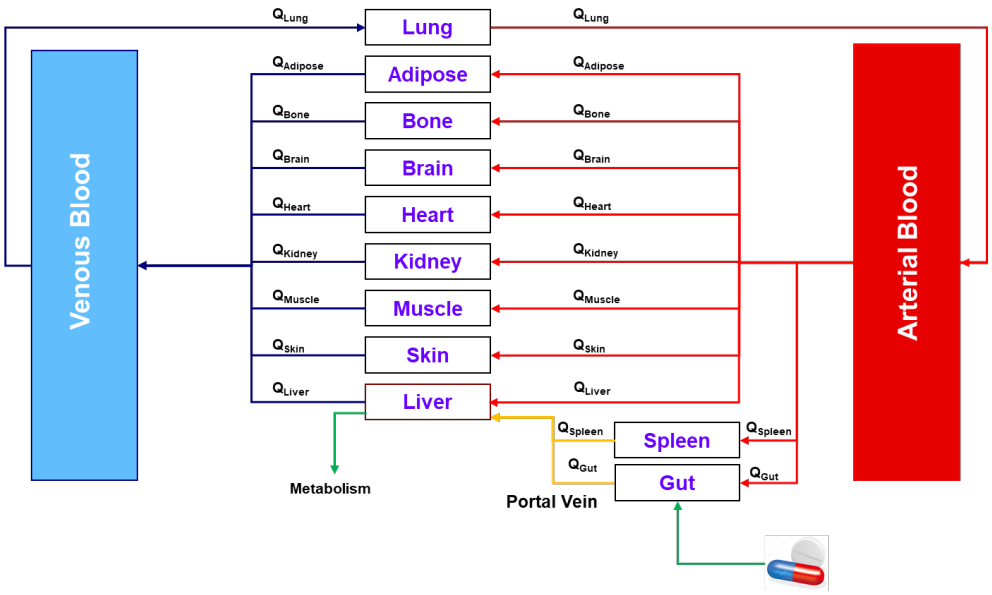

Figure 5. Schematic distribution model of full-body PBPK. Adapted from (Zhuang, Lu 2016).

Q, blood flow.

연세대학교
YONSEI UNIVERSITY

Table 3. Mean tissue volume and blood flow for healthy subjects aged between 18 and 65 years.

	Tissue volume (L)	**Blood flow (L/h)**
Adipose	23.44	22.10
Bone	3.36	16.22
Brain	1.27	38.92
Gut	1.16	3.24 (stomach) 34.11 (small intestine) 19.46 (villi) 14.65 (large intestine)
Heart	0.27	14.65
Kidney	0.30	58.26
Liver	1.46	21.08 (arterial) 65.82 (portal)
Lung	0.45	324.32

연세대학교
YONSEI UNIVERSITY

Muscle	24.15	46.73
Pancreas	0.11	3.24
Skin	2.46	16.22
Spleen	0.13	8.17
Plasma	3.03	-
Blood	4.83	-

연세대학교
YONSEI UNIVERSITY

Different theories were applied to predict the volume of distribution (V_{ss}) for each TZDs as accurately as possible relative to the observed value. V_{ss} is a hypothetical term defined as the volume of body fluid dissolving the drug at the same concentration as plasma, which was expressed as the ratio of the total quantity of drug in the body ($A_{b,ss}$) to the total concentration of drug in the plasma ($C_{p,ss}$) at steady state (Eq (6)).

$$V_{ss} = \frac{A_{b,ss}}{C_{p,ss}} \tag{6}$$

Theoretically, the total amount of drug in the body spreading into physiological compartments at steady state can be expressed as Eq (7).

$$A_{b,ss} = C_{p,ss} \cdot V_p + \sum_t C_{t,ss} \cdot V_t \tag{7}$$

Combining Eq (6) and (7), V_{ss} is also expressed by Eq (8):

$$V_{ss} = V_p + V_e \cdot E{:}P + \sum_t V_t \cdot P_{t:p} \tag{8}$$

Where, V_p, V_t, and V_e represent the volume of plasma, tissue, and erythrocyte.

The $P_{t:p}$, the tissue-partition coefficient is the ratio of the total drug concentration in each tissue ($C_{t,\,ss}$) to the plasma concentration ($C_{p,\,ss}$) at a steady state. In animal

연세대학교
YONSEI UNIVERSITY

study, the value can be measured directly after intravenous infusion. However, considering biochemical properties of a molecule at the cellular level, $P_{t:p}$ for human tissues can be generally estimated assuming the following hypothesis (Kazmi et al. 2013, Poulin, Theil 2002, Rodgers, Rowland 2007):

· Drugs are distributed homogeneously into plasma and tissues (a well-stirred distribution model)

· Drugs are transported via passive processes (blood perfusion limited model).

The Rodgers & Rowland prediction theory was applied for lobeglitazone and rosiglitazone due to their physicochemical properties as zwitterions. The Rodgers & Rowland method accounts for the dissolution of the drug into water, partitioning of unionized drugs into neutral lipids and phospholipids, electrostatic interactions between basic drugs and acidic phospholipids, and the interaction between extracellular proteins and bases, acids, neutrals molecules, and zwitterions (Figure 6). For drugs of moderate-to-strong bases ($pK_a \geq 7$) molecules and zwitterions (with at least one basic $pK_a \geq 7$), the distribution occurs predominantly binding to acidic phospholipids within the body (Eq (9)). For other compounds binding to extracellular proteins rather than acidic phospholipids is assumed to the predominant driver of distribution (Eq (10)).

연세대학교
YONSEI UNIVERSITY

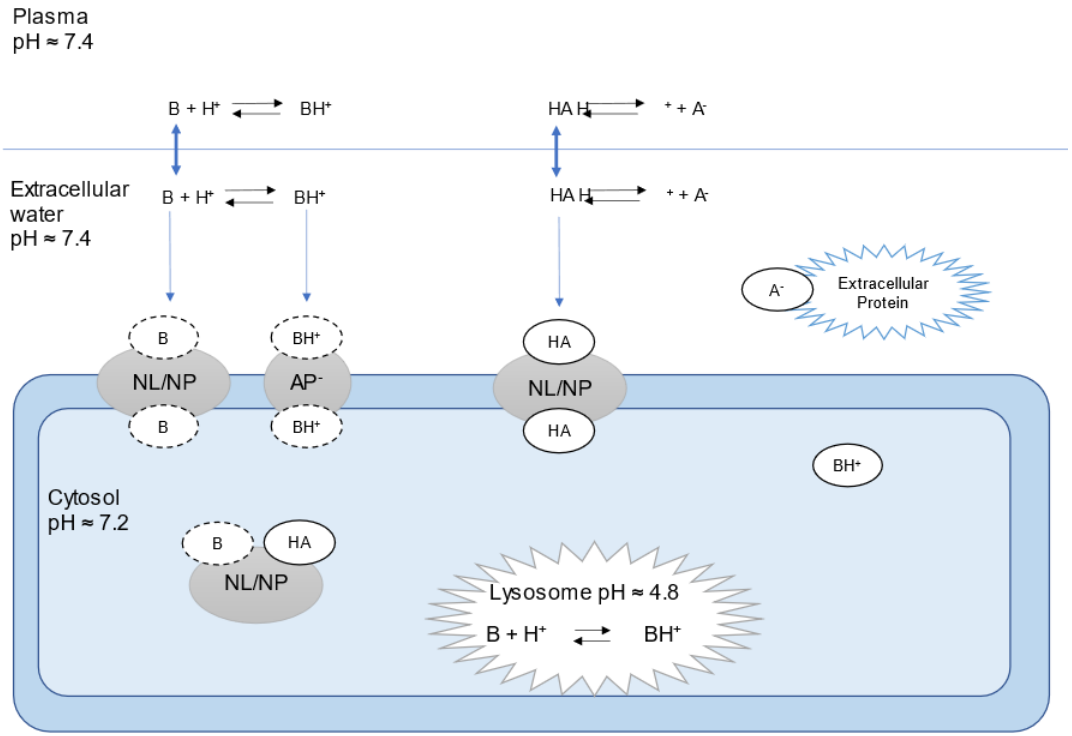

Figure 6. Illustration of a mechanistic distribution model at the cellular level, as suggested by Rodgers & Rowland.

Adapted from (Schmitt et al. 2021). NL, neutral lipid; NP, neutral phospholipid; B, base; A, acid; H, hydrogen.

연세대학교
YONSEI UNIVERSITY

$$K_{pu} = f_{EW} + \frac{X_{IW}}{X_{EW}} f_{IW} + \left(\frac{P \cdot f_{NL} + (0.3 \cdot P + 0.7) f_{NP}}{X_{EW}}\right) + \left(\frac{K_{a_{AP}} \cdot [AP^-]_t \cdot Y_{IW}}{X_{EW}}\right) \quad (9)$$

$$K_{pu} = f_{EW} + \frac{X_{IW}}{X_{EW}} f_{IW} + \left(\frac{P \cdot f_{NL} + (0.3 \cdot P + 0.7) f_{NP}}{X_{EW}}\right) + \left(K_{a_{PR}} \cdot [PR]_t\right) \quad (10)$$

Where, *f* is the fractional tissue volume; *ECF* is for extracellular fluid (extra cellular water); *ICF* is intracellular fluid (intracellular water); *P* is a partition coefficient for unionized molecules in the adipose determined by lipophilicity (log*P* or log*D*), *X* and *Y* represent for drug ionization; K_{aAP} was the affinity constant of a drug for acidic phospholipid (*AP*); $[AP^-]_t$ is the concentration of acidic phospholipid in the tissue *t*; and K_{aPR} is the affinity constant of a drug for extracellular tissue protein (PR). Because lobeglitazone and rosiglitazone bind mainly to albumin (≥99%), this study considered PR to comprise only plasma albumin. The Rodgers & Rowland method postulated that $P_{t:p}$ would be determined by f_u and K_{pu}. However, the Rodgers & Rowland method is known to have a tendency to overestimate $P_{t:p}$ of the brain and to underestimate that of the liver (Mathew et al. 2021). This is because the Rodgers & Rowland theory only accounts for the physicochemical properties (log*D* or log*P*, *pKa*, f_u, and *B/P*) of a drug without considering whether a drug hardly penetrates the blood-brain barrier or can be effluxed in the liver by active transporters. Therefore, $P_{t:p}$ of the brain for lobeglitazone and rosiglitazone were specifically calculated using the following equations (Clark 1999):

연세대학교
YONSEI UNIVERSITY

$$\log BB = -0.0156 \times PSA + 0.0548 \quad (11)$$

$$P_{t:p}\ (Brain) = B{:}P \times 10^{\log BB} \quad (12)$$

The $P_{t:p}$ of the brain obtained was 0.02 for lobeglitazone; 0.15 for rosiglitazone, which was similar to 0.16 estimated using the Rodgers & Rowland theory.

All $P_{t:p}$ values predicted using the Rodgers & Rowland method are also shown in Table 2. The estimated V_{ss} of lobeglitazone and rosiglitazone were 0.15 L/kg and 0.16 L/kg, respectively.

For pioglitazone, the expanded Rodgers & Rowland approach was applied to estimate $P_{t:p}$ and V_{ss} by considering the polarization of cell membranes, which would drive a force for cations to enter into the cells (Kazmi et al. 2013, Rodgers, Leahy, Rowland 2005a, b). In addition to the original Rodgers & Rowland approach, which only consider lipophilicity and acidity, the expanded approach includes the effects of other factors, such as pH in the *ECF* and *ICF*, the cellular membrane potential, dissociation, and ionization of molecules:

연세대학교
YONSEI UNIVERSITY

$$P_{t:P} = \Bigg[f_{ECF} + K_{a^{PR}} \cdot [PR]_{tissue} \{ f_{ECF} \cdot (1 + Y_{ICF}) + P_{NL} \cdot f_{NL} + P_{NP} \cdot f_{NP} + K_{a^{AP}} \cdot [AP]_{tissue} \cdot Y_{ICF} \} \cdot \frac{K_{p_{uu,uu}}}{1 + Y_{ECF}} \Bigg] \cdot f_u \quad (13)$$

Where, $K_{puu,uu}$ (the ratio of the unbound, unionized tissue concentration to the unbound, unionized plasma concentration) is defined using the Nernst equation:

$$K_{p_{uu,uu}} = \frac{C_{ICF}^{ub,ui}}{C_{ECF}^{ub,ui}} = \frac{1 + \sum_{i=1,2} \left[\frac{P^{ub,i}}{P^{ub,ui}} \frac{N_i}{e^{N_i} - 1} Y_{ECF}^{i} \right]}{1 + \sum_{i=1,2} \left[\frac{P^{ub,i}}{P^{ub,ui}} \frac{N_i}{e^{N_i} - 1} e^{N_i} Y_{ECF}^{i} \right]} \quad (14)$$

and $$Y_{ECF}^{i} = 10^{pKa - pH_{ECF}} \text{ or } Y_{ICF}^{i} = 10^{pKa - pH_{ICF}} \quad (15)$$

In the above equations, superscripts *ub*, and *ui* represented unbound and unionized, respectively. The $P_{t:p}$ of brain was also calculated using Eq (13)&(14) and estimated to be 0.303. The calculated V_{ss} for pioglitazone was 0.70 L/kg, which was out of the previously reported range 0.199–0.299 L/kg (Eckland, Danhof 2000). Therefore, the universal Kp scalar was set at 0.33 to obtain a V_{ss} value of 0.213 L/kg, which was close to the observed mean value of 0.253 L/kg.

TZDs are completely metabolized in the liver and excreted as metabolites through bile or urine; the fraction excreted unchanged in urine is negligible. In this study,

연세대학교
YONSEI UNIVERSITY

non-renal elimination of TZDs was assumed to be primarily mediated by hepatic enzymes. *In vitro* studies showed that lobeglitazone was depleted predominantly by recombinant human cytochrome P (*rhCYP*) 3A4, 2D6, and 2C19 (unpublished data). Hepatic intrinsic clearance (CL_{int}) at the enzyme level was back-calculated from the known oral clearance (CL_{po}) of 1.3 L/h in the retrograde enzyme kinetic model using Eq (16):

$$CL = CL_{Hepatic} + CL_{bile} + CL_{renal} \tag{16}$$

Where, *CL* denotes clearance, and the subscripts designate for hepatic, bile, and renal excretion. According to animal studies, because lobeglitazone is rarely excreted in urine and bile as the parent drug, thus CL_{renal} and CL_{bile} were set at 0 (Lee et al. 2015). CL_{po} is expressed as,

$$CL_{po} = CL_{Hepatic} = \frac{CL_{int} \times Q_H}{CL_{int} + Q_H} \times Active\ hepatic\ scalar \tag{17}$$

Where, CL_{int} is the clearance of a parent drug metabolized by hepatic enzymes.

$$CL_{int} = \left(\left(\sum (rhCYP \cdot phenotype\ acitivity)\right) + HLM\right) \times Liver\ weight \times HPGL \times Bodyweight \tag{18}$$

Where, *HPGL* is the hepatocellularity per gram liver, *HLM* represents the additional clearance of human liver microsomes.

연세대학교
YONSEI UNIVERSITY

The contributions of the individual CYP enzymes in lobeglitazone metabolism were estimated to be 33.4% for CYP3A4, 18.7% for CYP2D6, and 11.6% for CYP2C19. The retrograde model estimated the clearance of each enzyme to be 6.73, 14.97, and 1.36 μL/min/pmol for rhCYP3A4, rhCYP2C9, and rhCYP2D6, respectively. A previous study reported that the application of *in vitro–in vivo* extrapolation (IVIVE) with human microsome experimental values led to an underprediction of hepatic clearance by more than 6 times (Bowman, Benet 2019, Chiba, Ishii, Sugiyama 2009). These phenomena might be the result of not taking hepatic transporters into account in an *in vitro* CYP activity assay. Previous studies showed that strong interaction of lobeglitazone with hepatic uptake transporters, such as organic anion transporting polypeptides (OATPs) (Lee et al. 2015, Yim et al. 2017). Thus, the disposition of lobeglitazone in the liver could be underestimated. The possible error was simply calibrated by setting the active hepatic scalar at 7 due to lack of applicable experimental values for transporter activity. The *HLM* was also estimated via back-calculation (191.3 μL/min/mg).

For rosiglitazone, the general enzyme kinetic model by IVIVE was utilized to estimate the intrinsic clearance for individual CYP enzymes. Rosiglitazone was mainly depleted by CYP2C8 and CYP2C9 (Baldwin, Clarke, Chenery 1999, Bazargan et al. 2017). CL_{int} of rosiglitazone was calculated using following equations (Proctor, Tucker, Rostami-Hodjegan 2004):

연세대학교
YONSEI UNIVERSITY

$$CL_{int} = \left[\sum_{j=1}^{n} \frac{ISEF_j \times V_{max}(rCYP_j) \times X_j}{K_m(rCYP_j)}\right] \times MPPGL \times Liver\ weight \quad (19)$$

Where, j denotes the CYP isoforms, X_j is abundance of the relative CYP isoform in the population, *MPPGL* is milligrams of microsomal protein per gram of liver, and *ISEF* represents intersystem extrapolation factors defined as:

$$ISEF = \frac{V_{max_j}(system)}{V_{max_j}(rhCYP_j) \times CYP_j abundance(system)} \quad (20)$$

CYP_j *abundance* can be directly measured and depends on the experimental system. The estimated intrinsic clearance values of CYP2C19 and 2C9 for rosiglitazone were 169.6 and 84.6 μL/min/pmol, respectively. The *HLM* was estimated to be 35.7 μL/min/mg, and the active hepatic scalar was set at 1.

Similar to the lobeglitazone model, the retrograde enzyme kinetic model was also adopted for pioglitazone. The previous *in vitro* depletion assay estimated the contribution of CYP2C8 and CYP3A4 to be 56% and 37%, respectively (Jaakkola et al. 2006). The relative clearance of CYP2C8 and 3A4 was estimated at 2.38 and 0.24 μL/min/pmol with the *HLM* of 5.80 μL/min/mg by the retrograde enzyme kinetic model. Further, the active hepatic scalar of pioglitazone was set at 4 given

연세대학교
YONSEI UNIVERSITY

the possibility of its interaction with OATP1B1 according to the animal study (Chang et al. 2005).

연세대학교
YONSEI UNIVERSITY

2.2.2.Simulation of the PBPK Models

To validate the PBPK models, simulation was performed with 100 virtual individuals matched by age and sex and administered each TZD orally under fasting condition, and the results were compared with those of clinical trials (Table 4). The major PK parameters of these virtual trials were evaluated to validate the PBPK model of each TZD and compared to observed values.

The constructed and validated model of each TZD was simulated for 10 virtual healthy subjects in 10 trials with a defined age range (18–65 years) and sex (50% of males) for generalization.

연세대학교
YONSEI UNIVERSITY

Table 4. Summary of baseline demographics in clinical trials

TZDs	Dose	No. of subjects	Ages (years)*	Ratio of males (%)	References
Lobeglitazone	0.5 mg	12	38–52	84	
	2 mg	36	19–29	100	(Park et al. 2014)
	2 mg	11	20–26	0	(Kim et al. 2011)
Rosiglitazone	8 mg	4	40–65	100	(Cox et al. 2000)
	8 mg	10	22–26	100	(Park et al. 2004)
Pioglitazone	15 mg	12	20–27	75	(Jaakkola et al. 2005)
	30 mg	24	20–27	100	(Eckalnd, Danhof 2000)

Abbreviation: TZD, thiazolidinediones. *Minimum and maximum values.

연세대학교
YONSEI UNIVERSITY

2.3. The PBPK Models in Patients with Hepatic Impairment

The physiological parameters of patients with hepatic impairment were modulated based on a previous study (Johnson et al. 2010). The severity of hepatic impairment was stratified by Child-Pugh scores for bilirubin, albumin, prothrombin time, encephalopathy, and ascites. The physiological parameters, including liver volume, activities of CYPs, albumin concentration in the plasma, hematocrit, and blood flow were altered in accordance with the Child-Pugh classification (Table 5). Decreased liver size with increasing severity of hepatic impairment according to the Child-Pugh classification reflects the functional reserve of the liver. The reduced expression of CYPs in severe hepatic impairment would indicate the decreased CYP activity. The significantly decreased albumin level in hepatic impairment accounts for the estimation of the unbound fraction of drug. Because TZDs binds to plasma albumin more than 99%, the unbound fraction in hepatic impairment (f_{uHI}) could be estimated by following in each patient:

$$f_{u,HI} = \frac{1}{1 + \frac{(1 - f_u) \times [Albumin]_{HI}}{[Albumin] \times f_u}} \quad (21)$$

Where, f_u denotes the unbound fraction of TZDs in the healthy subjects, *[Albumin]* is the average concentration of albumin in the population, and *HI* stands for hepatic impairment. The decreased hematocrit level in patients with hepatic impairment was included as a the physiological parameter in B:*P* calculations. Changes in blood flow

연세대학교
YONSEI UNIVERSITY

reflected hyperdynamic circulation due to shunting in patients with hepatic impairment.

연세대학교
YONSEI UNIVERSITY

Table 5. Characteristics of the virtual population with hepatic impairment.

Physiological parameters	Healthy population	Child-Pugh Class		
		A	B	C
Liver volume fraction	1.0	0.81	0.65	0.53
CYP (pmol/mg)				
2C8	24	16.6	12.5	7.90
2C9	73	50.4	38.0	24.1
2C19	14	4.50	3.60	1.70
2D6	8.0	6.10	2.60	0.84
3A4	137	80.8	53.2	34.2
Albumin (g/L)	44.7	41.1	33.9	26.3
Hematocrit (%)	45.0	36.6	32.9	31.9
Cardiac output (L/h)	306	355	403	431
Portal blood flow (L/h)				
males	58.2	52.9	36.9	32.2
females	65.8	59.9	41.7	36.4
Hepatic arterial blood flow (L/h)	19.9	28	32.3	38.1
Villous blood flow (L/h)	18.4	23.7	28.0	36.6

Abbreviation: CYP, Cytochrome P.

연세대학교
YONSEI UNIVERSITY

2.3.1.Simulation of the PBPK Models

One hundred virtual individuals (10 subjects in 10 trials) were simulated in each Child-Pugh class. The age range was defined from 18 to 65 years, and the ratio of male and female was set to 50:50 for generalization.

The virtual populations were within the defined ranges of age and sex and were randomly selected by Monte Carlo statistical sampling in Weibull distribution statistics.

2.3.2.Multiple-dose Simulation

Multiple-dose simulations were performed with the developed PBPK models of TZDs in healthy subjects and patients with hepatic impairment classified according to the Child-Pugh system because these antidiabetic drugs are taken for long periods. When considering the recommended dosage of TZDs, the simulations were performed at the given dose (0.5 mg for lobeglitazone, 8 mg for rosiglitazone, and 15 mg for pioglitazone) once daily for 10 days. The virtual population of the simulation was within the defined age range between 18 and 65 years, with a 50:50 male: female ratio. The concentration–time curves were compared for Child-Pugh A, B, and C patients and healthy subjects for a given duration.

연세대학교
YONSEI UNIVERSITY

2.4. Evaluation and Simulation of the PBPK Models

In general, the error in the predicted PK parameters relative to the observed values was estimated using Eq (22) (Matsumoto et al. 2019):

$$Prediction\ Error\ (PE) = \frac{X_{predicted}}{X_{observed}} \quad (22)$$

Where $X_{predicted}$ is the simulated geometric mean of C_{max}, AUC_{last}, or AUC_{inf} for 10 clinical trials of 10 virtual individuals (100 simulations); $X_{observed}$ represents the observed geometric mean values estimated in the clinical trial. When PE is in the range of 0.5-2.0, The PBPK model was acceptable when the PE would be in the range of 0.5–2.0; it was optimized when the PE was in the range of 0.80–1.25. The model was considered inappropriate for prediction when the PE was less than 0.5 or more than 2.0.

Additionally, for all available data the visual predictive checks were performed for the predicted concentration–time curves to determine whether the mean observed values were within the 95% confidence intervals.

연세대학교
YONSEI UNIVERSITY

3. Results

3.1. Validation in Healthy Subjects

The PBPK model of lobeglitazone was simulated to compare with the observed age- and sex-matched data. The observed mean values were within the 95% confidence intervals (Figure 7, Appendix 2). The prediction errors were within the 0.80–1.25, indicating equivalence. As previous studies had demonstrated linearity of PK parameters for up to 2 mg of lobeglitazone, model validation was also performed for the oral administration of 2 mg of lobeglitazone (Kim et al. 2011). The model was acceptable with fold error ranges between 0.5 and 2.0 compared to clinical trial data for even a high dose of lobeglitazone in both males and females (Table 6). The PBPK model of rosiglitazone and pioglitazone was also validated in a healthy virtual population and compared to clinical trial data (Figure 8&9). The predicted major PK parameters for frequently used doses were within the equivalence range between 0.80 and 1.25 (Table 7).

연세대학교
YONSEI UNIVERSITY

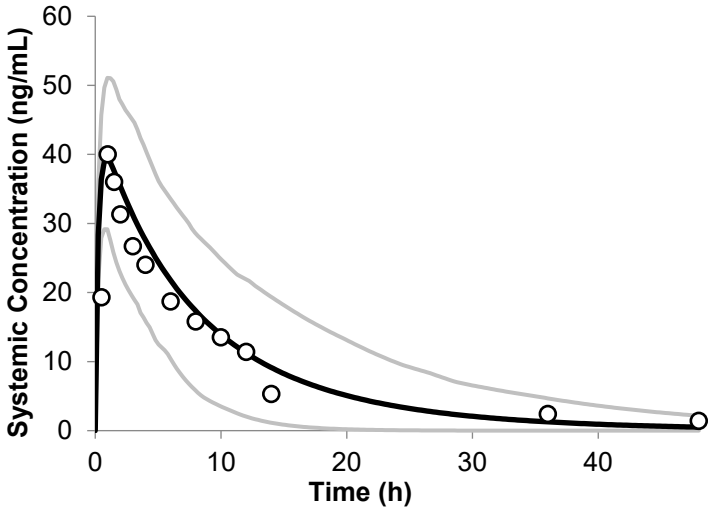

Figure 7. Visual predictive check for 0.5 mg lobeglitazone in healthy volunteers.

Solid line represents the mean concentration–time curve in the virtual population. Dots represent the observed mean concentrations.

연세대학교
YONSEI UNIVERSITY

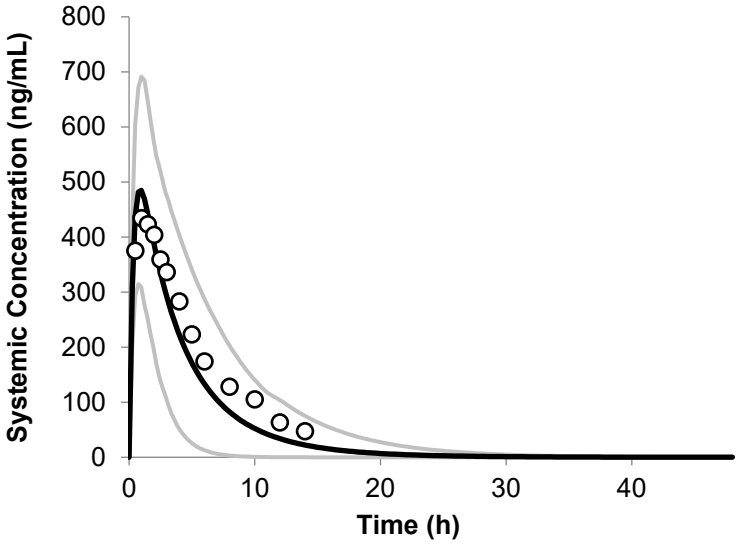

Figure 8. Visual predictive check of 8 mg rosiglitazone in healthy volunteers.

Solid line represents the mean concentration–time curve in the virtual population. Dots represent the observed mean concentrations.

연세대학교
YONSEI UNIVERSITY

(a)

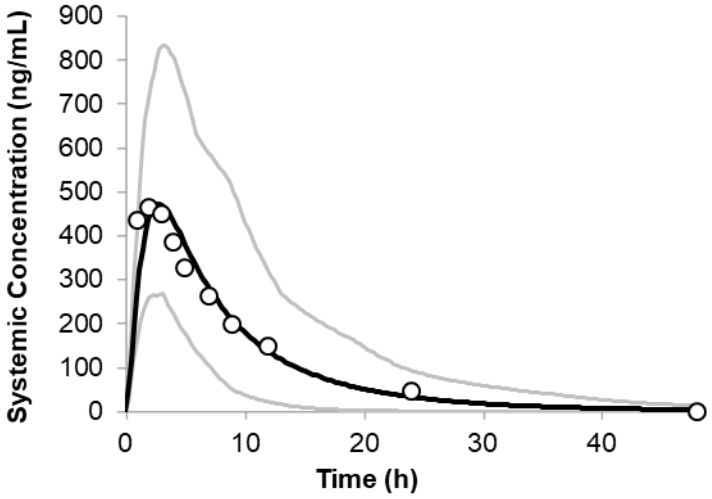

(b)

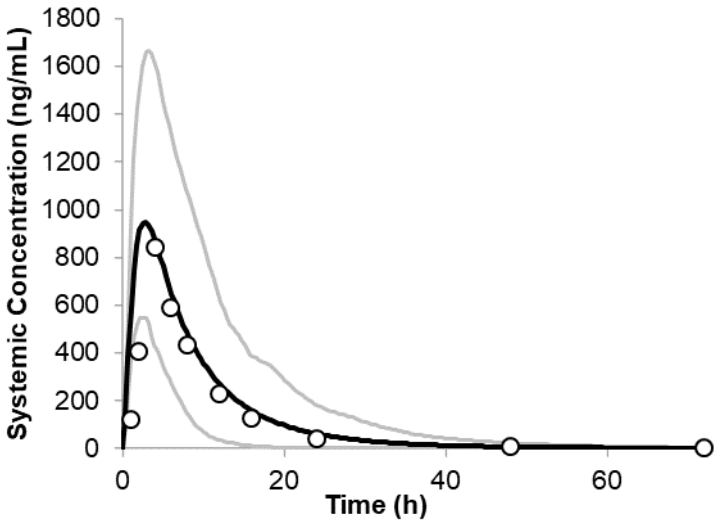

Figure 9. Visual predictive check of (a) 15 mg and (b) 30 mg pioglitazone in healthy volunteers.

Solid lines represent the mean concentration–time curves in the virtual population. Dots represent the observed mean concentration.

연세대학교
YONSEI UNIVERSITY

Table 6. The observed and predicted PK parameters of lobeglitazone in healthy volunteers.

Dose	PK parameter	Observation	Prediction	PE
0.5 mg	C_{max} (ng/mL)	47.71 (8.22)	40.20 (7.86)	0.84
	AUC_{last} (h·ng/mL)	408.01 (138.12)	394.01 (159.23)	0.97
	AUC_{inf} (h·ng/mL)	428.62 (156.43)	402.03 (173.33)	0.94
	T_{max} (h)*	1.00 (1.00–1.50)	0.90 (0.55–1.30)	
2.0 mg (Males)	C_{max} /dose (ng/mL/mg)	86.7 (20.5)	77.8 (18.67)	0.90
	AUC_{inf} /dose (h·ng/mL/mg)	1004.8 (337.2)	706.6 (277.34)	0.70
	T_{max} (h)*	1.00 (1.00–2.00)	0.95 (0.55–1.35)	
2.0 mg (Females)	C_{max} /dose (ng/mL/mg)	107.4 (28.2)	85.09 (19.15)	0.79
	AUC_{inf} /dose (h·ng/mL/mg)	1125.6 (360.6)	780.43 (327.10)	0.69
	T_{max} (h)*	1.00 (0.48–4.00)	0.90 (0.45–1.25)	

Abbreviation: C_{max}, peak concentration; AUC_{last}, the area under concentration-time curve at the last quantifiable time; AUC_{inf}, the area under concentration-time curve extrapolated to the infinite; T_{max}, time to peak concentration; PE, prediction error. All data shown as mean values with standard deviation. * Data shown median with minimum and maximum values.

연세대학교
YONSEI UNIVERSITY

Table 7. The observed and predicted PK parameters of rosiglitazone and pioglitazone in healthy volunteers.

Dose and drugs	PK parameter	Observation	Prediction	PE
8 mg[a] Rosiglitazone (Males)	C_{max} (ng/mL)	603 (332)	516 (93)	0.86
	AUC_{inf} (h·ng/mL)	2930 (473)	2572 (1265)	0.88
	T_{max} (h)*	0.75 (0.75–1.00)	0.65 (0.35–1.05)	
8 mg[b] Rosiglitazone (Males)	C_{max} (ng/mL)	538 (117)	490 (114)	0.91
	AUC_{last} (h·ng/mL)	2676 (405)	2353 (1114)	0.88
	T_{max} (h)*	0.80 (0.50–2.5)	0.90 (0.50–1.20)	
15 mg Pioglitazone (67% of males)	C_{max} (ng/mL)	518 (224)	488 (170)	0.94
	AUC_{last} (h·mg/L)	5.14 (2.30)	4.69 (2.41)	0.91
	AUC_{inf} (h·ng/mL)	5.25 (2.23)	4.73 (2.47)	0.90
	T_{max} (h)*	2.00 (1.00–4.00)	2.80 (1.45–4.05)	
30 mg Pioglitazone	C_{max} (ng/mL)	715 (216)	1008 (349)	1.41
	AUC_{last} (h·ng/mL)	7652 (3139)	10340 (5760)	1.35

연세대학교
YONSEI UNIVERSITY

(Males)	T_{max} (h)*	2.5 (1.18)	2.85 (1.35–4.00)

Abbreviation: C_{max}, peak concentration; AUC_{last}, the area under concentration-time curve at the last quantifiable time; AUC_{inf}, the area under concentration-time curve extrapolated to the infinite; T_{max}, time to peak concentration; PE, prediction error. All data shown as mean values with standard deviation. * Data shown median with minimum and maximum values. [a] indicates the study results of Cox et al (2000). [b] indicates the study results of Park (2004).

연세대학교
YONSEI UNIVERSITY

3.2. Simulation in Hepatic Impairment Classified by the Child-Pugh Classification System

For lobeglitazone, the observed data of Child-Pugh class A and B patients were used to evaluate the developed PBPK model in hepatically impaired patients. Thus, validation of the lobeglitazone PBPK model in these patients was performed with 100 virtual, age- and sex-matched individuals to the clinical trials. For Child-Pugh Class A and B patients, all observed mean values overlapped with the lower and upper 95% confidence intervals in the concentration–time curves, and the fold errors of the major PK parameters were within the acceptable range (Figure 10, Table 8).

연세대학교
YONSEI UNIVERSITY

(a)

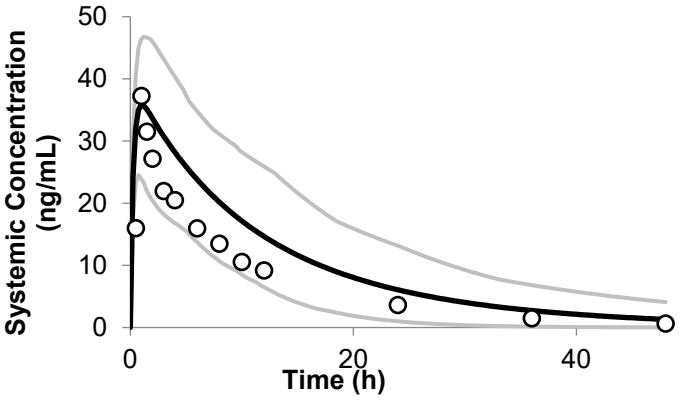

(b)

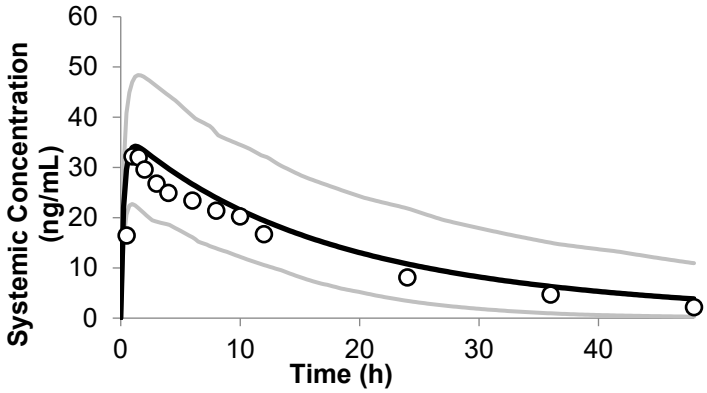

Figure 10. Visual predictive check of 0.5 mg lobeglitazone in patients with (a) Child-Pugh Class A (b) Child-Pugh Class B.

Solid lines represent the mean concentration–time curves in the virtual population. Dots represent the observed mean concentration.

연세대학교
YONSEI UNIVERSITY

Table 8. The observed and predicted PK parameters of lobeglitazone in patients with Child-Pugh Class A and B

Child-Pugh Class	PK parameter	Observation	Prediction	Fold Error
A	C_{max} (ng/mL)	38.53 (6.74)	36.54 (7.38)	0.94
	AUC_{last} (h·ng/mL)	318.00 (81.8)	472.53 (187.01)	1.49
	AUC_{inf} (h·ng/mL)	325.80 (83.00)	499.43 (221.66)	1.53
	T_{max} (h)	1.00 (1.00–1.50)	1.03 (0.65–1.60)	
	$t_{1/2}$ (h)	7.80 (1.52)	8.93 (4.14)	
	CL/F	1.65 (0.57)	1.23 (0.57)	
B	C_{max} (ng/mL)	33.79 (9.38)	37.15 (7.28)	1.10
	AUC_{last} (h·ng/mL)	539.70 (209.20)	645.95 (235.36)	1.20
	AUC_{inf} (h·ng/mL)	580.30 (225.70)	730.06 (327.97)	1.26
	T_{max} (h)	1.50 (1.00–1.05)	1.30 (0.80–1.80)	
	$t_{1/2}$ (h)	12.52 (2.3)	12.80 (5.69)	
	CL/F	0.97 (0.39)	0.84 (0.39)	

연세대학교
YONSEI UNIVERSITY

Abbreviation: C_{max}, peak concentration; AUC_{last}, area under concentration-time curve at the last quantifiable time; AUC_{inf}, the area under concentration-time curve extrapolated to the infinite; T_{max}, time to peak concentration; t1/2, half-life; CL/F, the apparent clearance; PE, prediction error. All data shown as mean values with standard deviation. * Data shown median with minimum and maximum values

연세대학교
YONSEI UNIVERSITY

After verification of the PBPK model for lobeglitazone in hepatically impaired patients, simulation of the model was performed in the virtual population with hepatic impairment stratified by the Child-Pugh classification system. The concentration–time curves showed that the values of C_{max} were not significantly different in the patient group, whereas the elimination rates were slightly delayed in the Child-Pugh B and C patients (Figure 11). Compared to the healthy subjects, C_{max} values in the hepatically impaired patients were greater than 0.95 but not different; the geometric mean ratio (GMR) was ~1. The GMRs of AUC_{last} in the Child-Pugh B and C patients were 1.80 and 1.94, respectively (Table 9).

연세대학교
YONSEI UNIVERSITY

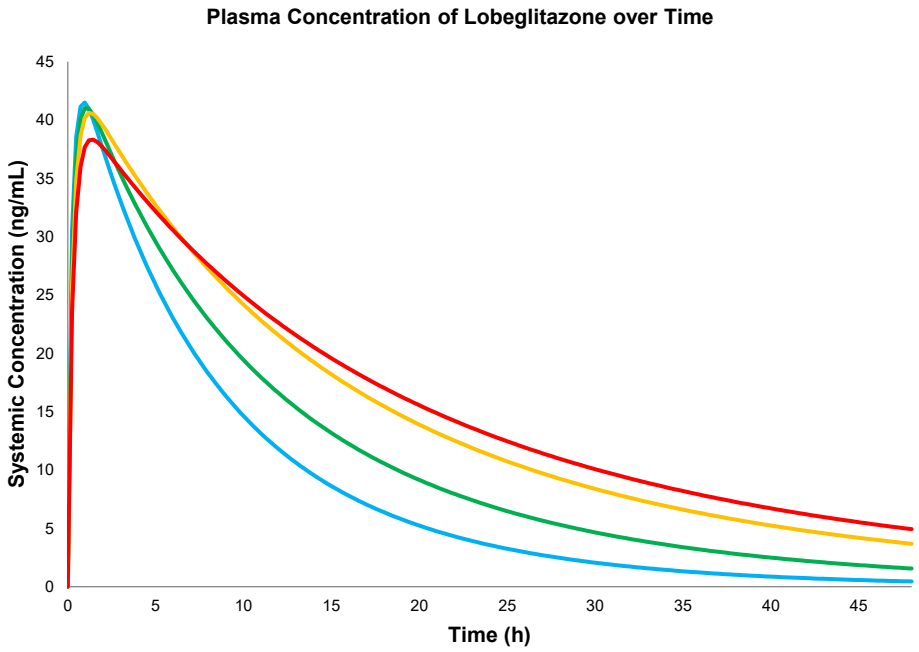

Figure 11. The concentration–time curve of 0.5 mg lobeglitazone in virtual populations.

The blue solid line represents the healthy population; green represents Child-Pugh A; yellow Child-Pugh B; and red Child-Pugh C.

연세대학교
YONSEI UNIVERSITY

Table 9. Comparison of PK parameters for 0.5 mg lobeglitazone in virtual population.

PK parameter	Healthy subjects	Child-Pugh A (Mild HI)	GMR	Child-Pugh B (Moderate HI)	GMR	Child-Pugh C (Severe HI)	GMR
C_{max} (ng/mL)	41.98 (9.38)	41.38 (9.45)	0.98	40.78 (8.90)	0.97	38.44 (8.06)	0.92
AUC_{last} (h·ng/mL)	408.97 (179.37)	547.05 (229.55)	1.36	715.90 (270.97)	1.80	765.87 (267.77)	1.94
AUC_{inf} (h·ng/mL)	414.95 (188.07)	576.97 (272.07)	1.39	810.8 (383.80)	1.96	913.83 (425.68)	2.21
T_{max} (h)*	0.90 (0.50–1.40)	1.00 (0.60–1.60)		1.30 (0.80–1.80)		1.40 (0.90–1.90)	
$t_{1/2}$ (h)	6.12 (2.36)	8.93 (3.82)		12.88 (5.62)		15.53 (6.86)	
CL/F	1.50 (0.76)	1.06 (0.49)	0.71	0.81 (0.33)	0.54	0.67 (0.33)	0.45
V_{ss} (L/kg)	0.15	0.15		0.16		0.17	
F	0.96	0.97		0.97		0.98	

연세대학교
YONSEI UNIVERSITY

Accumulation Index	1.09	1.20	1.40	1.54

Abbreviation: C_{max}, peak concentration; AUC_{last}, area under concentration-time curve at the last quantifiable time; AUC_{inf}, the area under concentration-time curve extrapolated to the infinite; T_{max}, time to peak concentration; t1/2, half-life; CL/F, the apparent clearance; V_{ss}, the volume of distribution; *F*, oral bioavailability; GMR, geometric mean ratio. All data shown as mean values with standard deviation. * Data shown median with minimum and maximum values.

연세대학교
YONSEI UNIVERSITY

No data were available to verify the PBPK models for rosiglitazone and pioglitazone in patients with hepatic impairment according to the severity. Thus, the simulation results in 100 virtual populations were compared to the trends of PK changes reported by the previous studies. The PBPK models of rosiglitazone and pioglitazone verified in healthy subjects were also simulated in patients with hepatic impairment by severity. For rosiglitazone, C_{max} decreased slightly with increasing severity, although the decrease was not clinically significant. Compared to healthy subjects, the GMR was 1.00 for Child-Pugh A, 0.92 for Child-Pugh B, and 0.81 for Child-Pugh C. However, the AUCs increased significantly. For Child-Pugh class C, the GMRs of the AUCs were greater than 2.0 (Figure 12, Table 10). The C_{max} values for pioglitazone were not significantly different for healthy subjects and patients with hepatic impairment regardless of severity. However, T_{max} values were slightly delayed with increasing severity of hepatic impairment. The AUCs of the Child-Pugh B and C patients showed GMRs were more than 2. Thus, the apparent clearance was significantly decreased in patients with hepatic impairment (Figure 13, Table 11).

연세대학교
YONSEI UNIVERSITY

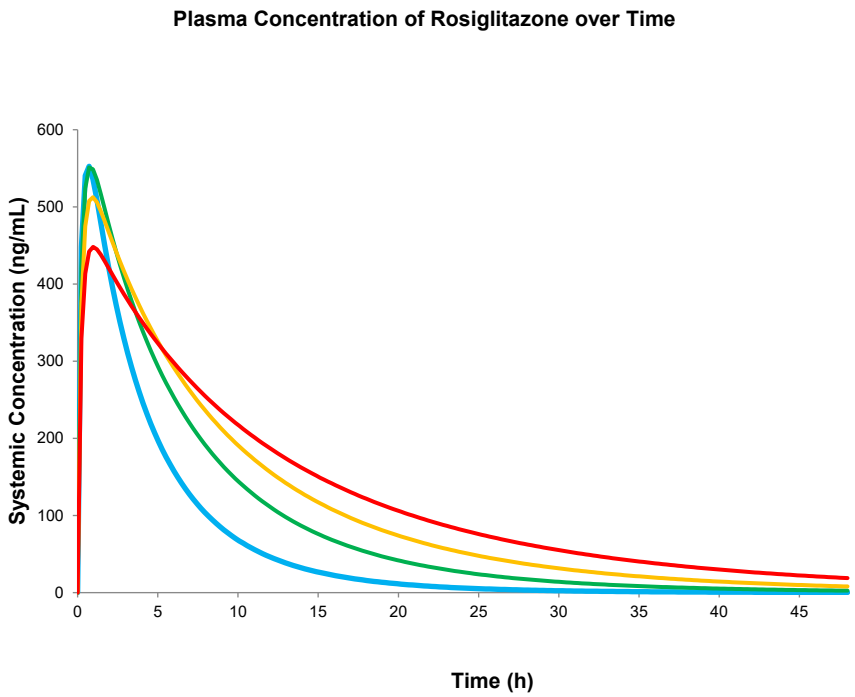

Figure 12. The concentration–time curve of 8 mg rosiglitazone in virtual populations.

The blue solid line represents the healthy population; green represents Child-Pugh A; yellow Child-Pugh B; and red Child-Pugh C.

연세대학교
YONSEI UNIVERSITY

Table 10. Comparison of PK parameters for 8 mg rosiglitazone in virtual population.

PK parameter	Healthy subjects	Child-Pugh A (Mild HI)	GMR	Child-Pugh B (Moderate HI)	GMR	Child-Pugh C (Severe HI)	GMR
C_{max} (ng/mL)	560 (133)	559 (136)	1.00	517 (120)	0.92	452 (100)	0.81
AUC_{last} (h·ng/mL)	2802 (1464)	4331 (2246)	1.54	5360 (2681)	1.93	6159 (2854)	2.26
AUC_{inf} (h·ng/mL)	2805 (1468)	4365 (2312)	1.55	5485 (2885)	1.96	6524 (3343)	2.35
T_{max} (h)*	0.65 (0.35–1.35)	0.83 (0.50–1.20)		0.95 (0.55–1.30)		1.00 (0.60–1.40)	
$t_{1/2}$ (h)	2.83 (1.32)	4.65 (2.16)		6.47 (2.93)		9.12 (3.95)	
CL/F	3.92 (2.65)	2.57 (1.89)	0.65	2.01 (1.40)	0.51	1.65 (1.08)	0.42
V_{ss} (L/kg)	0.16	0.17		0.19		0.23	
F	0.93	0.95		0.95		0.96	

연세대학교
YONSEI UNIVERSITY

Accumulation Index	1.01	1.04	1.10	1.21

Abbreviation: C_{max}, peak concentration; AUC_{last}, area under concentration-time curve at the last quantifiable time; AUC_{inf}, the area under concentration-time curve extrapolated to the infinite; Tmax, time to peak concentration; t1/2, half-life; CL/F, the apparent clearance; V_{ss}, the volume of distribution; F, oral bioavailability; GMR, geometric mean ratio. All data shown as mean values with standard deviation. * Data shown median with minimum and maximum values.

연세대학교
YONSEI UNIVERSITY

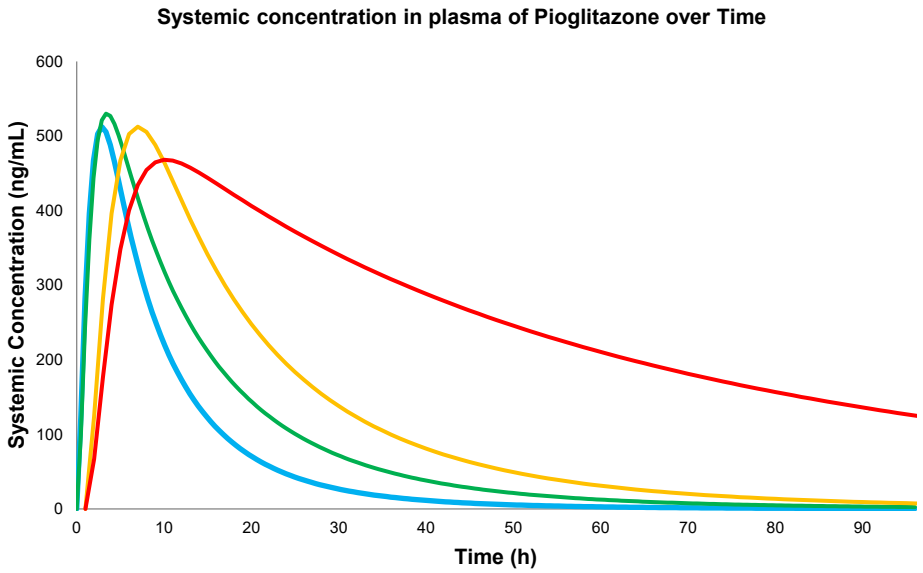

Figure 13. The concentration–time curve of 15 mg pioglitazone in virtual populations.

The blue solid line represents the healthy population; green represents Child-Pugh A; yellow Child-Pugh B; and red Child-Pugh C.

연세대학교
YONSEI UNIVERSITY

Table 11. Comparison of PK parameters for 15 mg pioglitazone in virtual population.

PK parameter	Healthy subjects	Child-Pugh A (Mild HI)	GMR	Child-Pugh B (Moderate HI)	GMR	Child-Pugh C (Severe HI)	GMR
C_{max} (ng/mL)	526 (191)	544 (199)	1.03	5.40 (191)	1.03	477 (164)	0.91
AUC_{last} (h·ng/mL)	5642 (3272)	8429 (4808)	1.48	12527 (7225)	2.19	15429 (8307)	2.76
AUC_{inf} (h·ng/mL)	5651 (3291)	8506 (4935)	1.49	13012 (7952)	2.24	17098 (10376)	2.96
T_{max} (h)*	2.85 (1.35–4.05)	3.40 (1.35–4.90)		3.85 (1.50–5.60)		4.25 (1.60–6.15)	
$t_{1/2}$ (h)	6.90 (2.74)	11.1 (9.82)		14.8 (7.85)		22.3 (12.4)	
CL/F	3.94 (3.44)	2.71 (2.38)	0.69	1.83 (1.72)	0.46	1.38 (1.28)	0.35
V_{ss} (L/kg)	0.22	0.23		0.26		0.32	
F	0.83	0.84		0.87		0.88	

연세대학교
YONSEI UNIVERSITY

Accumulation Index	1.11	1.30	1.50	1.92

Abbreviation: C_{max}, peak concentration; AUC_{last}, area under concentration-time curve at the last quantifiable time; AUC_{inf}, the area under concentration-time curve extrapolated to the infinite; Tmax, time to peak concentration; t1/2, half-life; CL/F, the apparent clearance; V_{ss}, the volume of distribution; F, oral bioavailability; GMR, geometric mean ratio. All data shown as mean values with standard deviation. * Data shown median with minimum and maximum values.

연세대학교
YONSEI UNIVERSITY

3.2.1. Multiple-dose Simulations

The concentration–time curves were simulated assuming multiple dosing with the developed PBPK models of lobeglitazone, rosiglitazone, and pioglitazone (Figure 14, 15, 16). Similar to the results for single–dose administration, exposure of multiple study showed the significant increases in patient with hepatic impairment by severity.

연세대학교
YONSEI UNIVERSITY

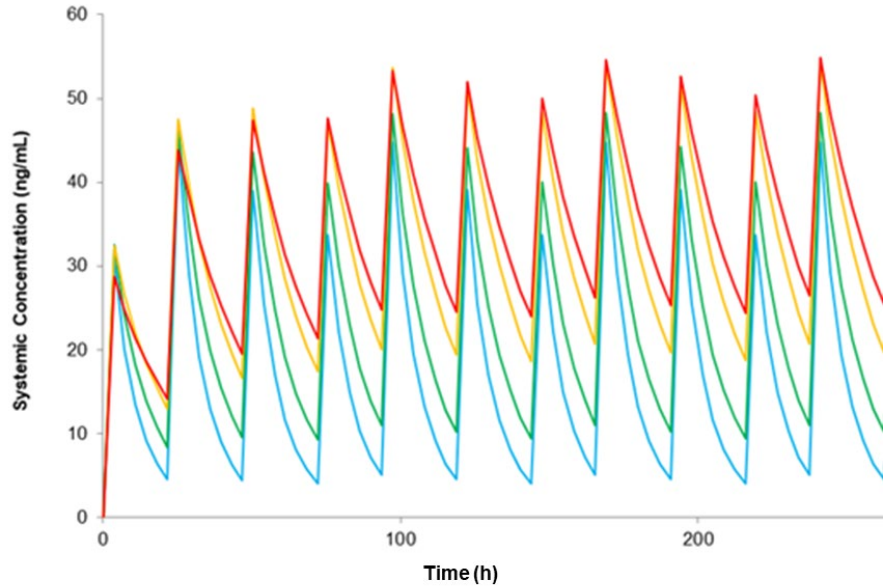

Figure 14. The concentration–time curve of 0.5 mg lobeglitazone once daily for 10 days in virtual populations.

The blue solid line represents the healthy population; green represents Child-Pugh A; yellow Child-Pugh B; and red Child-Pugh C.

연세대학교
YONSEI UNIVERSITY

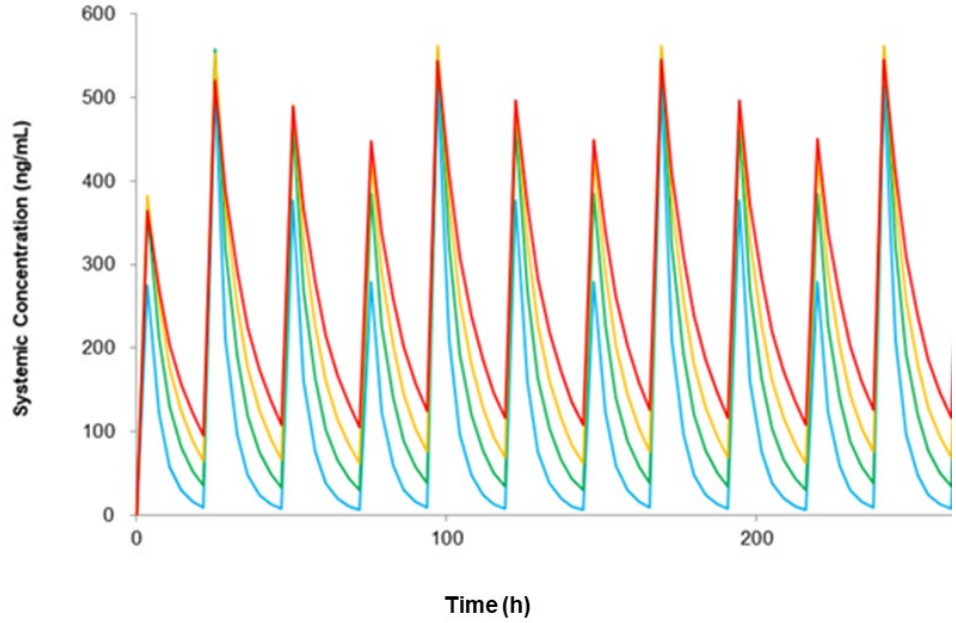

Figure 15. The concentration–time curve of 8 mg rosiglitazone once daily for 10 days in virtual populations.

The blue solid line represents the healthy population; green represents Child-Pugh A; yellow Child-Pugh B; and red Child-Pugh C.

연세대학교
YONSEI UNIVERSITY

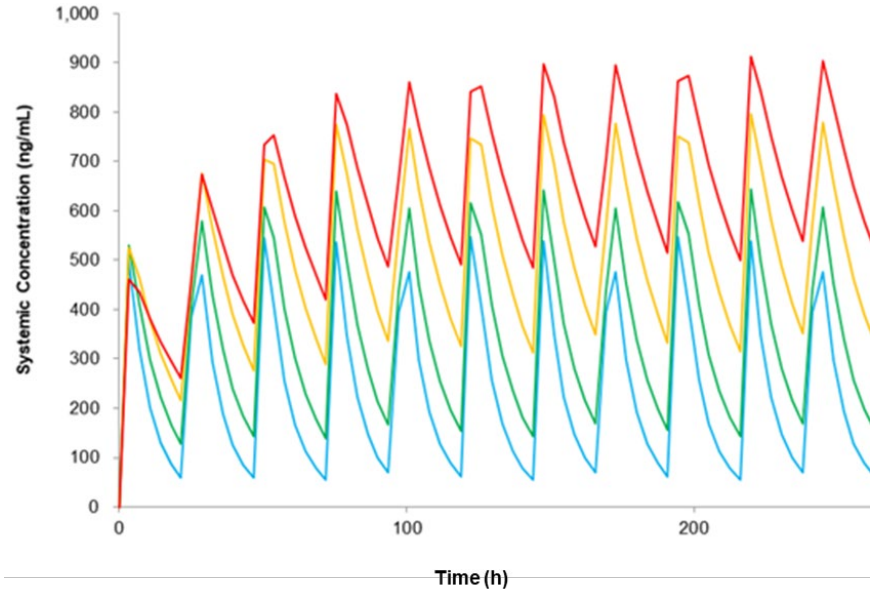

Figure 16. The concentration–time curve of 15 mg pioglitazone once daily for 10 days in virtual populations.

The blue solid line represents the healthy population; green represents Child-Pugh A; yellow Child-Pugh B; and red Child-Pugh C.

연세대학교
YONSEI UNIVERSITY

3.3. Additional Analysis of Simulation Results

3.3.1. Unbound Fractions of TZDs in Patients with Hepatic Impairment

As TZDs are known to be ultra-high bound to albumin (>99%), the exact unbound fractions in the plasma were hardly measured and the reported values varied because of low reproducibility. A remarkable advantage of PBPK modeling and simulation is the estimation of parameters using mathematical strategies because of technical limitations of experimental determination. Unbound concentrations over time of lobeglitazone, rosiglitazone, and pioglitazone were estimated in the virtual population according to the Child-Pugh classification system. The unbound concentrations of lobeglitazone in the Child-Pugh class A patients were comparable to those in the healthy subjects, with a GMR of C_{max} at 1.13 and that of AUC_{last} at 1.51. For lobeglitazone, the unbound C_{max} value increased by the severity of hepatic impairment. Notably, AUC_{last} increased by more than 3-fold in the Child-Pugh class C patients (Figure 17, Table 12).

연세대학교
YONSEI UNIVERSITY

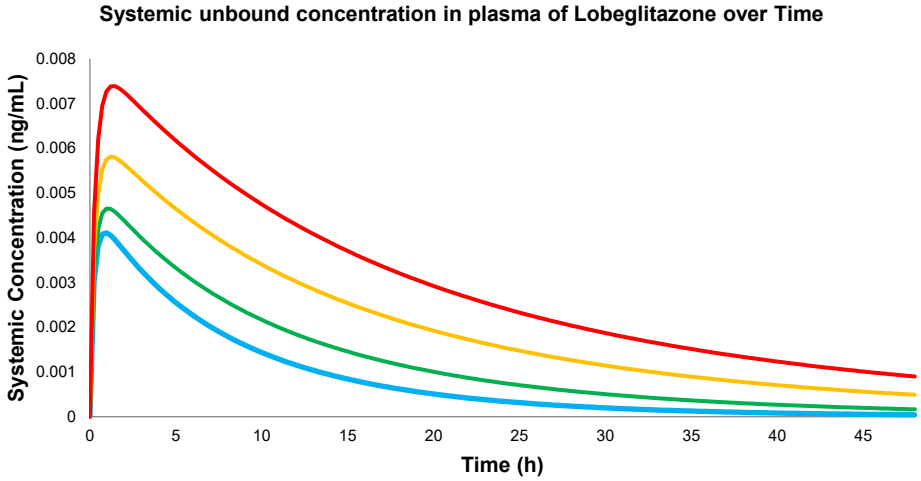

Figure 17. The unbound concentration–time curve of lobeglitazone in virtual populations.

The blue solid line represents the healthy population; green represents Child-Pugh A; yellow Child-Pugh B; and red Child-Pugh C.

Table 12. PK parameters of unbound lobeglitazone in virtual populations

PK parameters	Healthy	Child-Pugh A	GMR	Child-Pugh B	GMR	Child-Pugh C	GMR
C_{max} (pg/mL)	4.109	4.652	1.13	5.809	1.41	7.389	1.80
AUC_{last} (h·pg/mL)	39.991	60.676	1.51	99.864	2.50	144.585	3.62
T_{max} (h)	0.96	0.96		1.20		1.44	

Abbreviations: C_{max}, peak concentration; AUC_{last}, area under concentration-time curve at the last quantifiable time; T_{max}, time to C_{max}; GMR, geometric mean ratio; All data shown as mean values with standard deviation.

연세대학교
YONSEI UNIVERSITY

For rosiglitazone, the unbound concentrations over time in the Child-Pugh class A patients were comparable to those in the healthy subjects, with a GMR of C_{max} at 1.14 and of AUC_{last} at 1.78. However, the GMR of AUC_{last} increased by 3 times and 5 times in the Child-Pugh B and C patients (Figure 18, Table 13).

The unbound concentrations over time for pioglitazone showed a similar trend to that of rosiglitazone. In the Child-Pugh class A patients, the unbound concentration was comparable to that in the healthy subjects, with a GMR of C_{max} at 1.14 and of AUC_{last} at 1.78. In contrast, the AUC_{last} in the Child-Pugh class B and C patients were increased by 3-fold and 6-fold, respectively (Figure 19, Table 14).

연세대학교
YONSEI UNIVERSITY

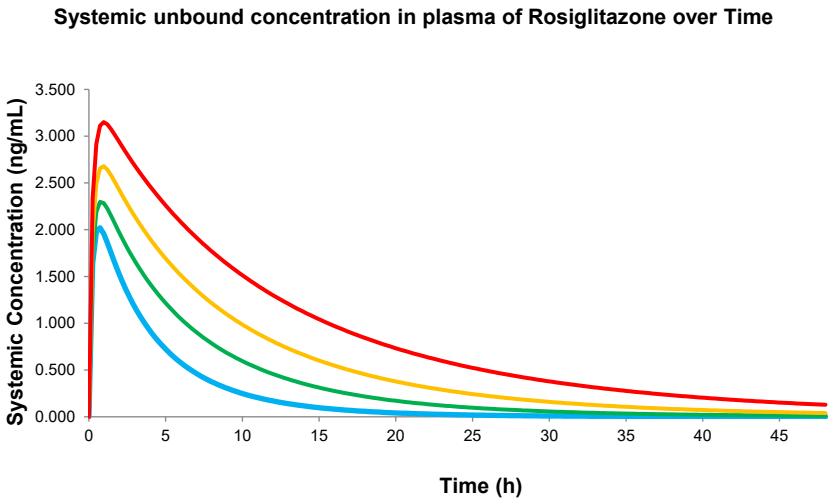

Figure 18. The unbound concentration–time curve of rosiglitazone in virtual populations.

The blue solid line represents the healthy population; green represents Child-Pugh A; yellow Child-Pugh B; and red Child-Pugh C.

Table 13. PK parameters of unbound rosiglitazone in virtual populations

PK parameters	Healthy	Child-Pugh A	GMR	Child-Pugh B	GMR	Child-Pugh C	GMR
C_{max} (ng/mL)	1.05	1.23	1.17	1.54	1.48	1.84	1.77
AUC_{last} (h·ng/mL)	11.537	19.524	1.73	36.288	3.23	60.161	5.66
T_{max} (h)	2.88	3.36		3.84		4.32	

Abbreviations: C_{max}, peak concentration; AUC_{last}, area under concentration-time curve at the last quantifiable time; T_{max}, time to C_{max}; GMR, geometric mean ratio; All data shown as mean values with standard deviation.

연세대학교
YONSEI UNIVERSITY

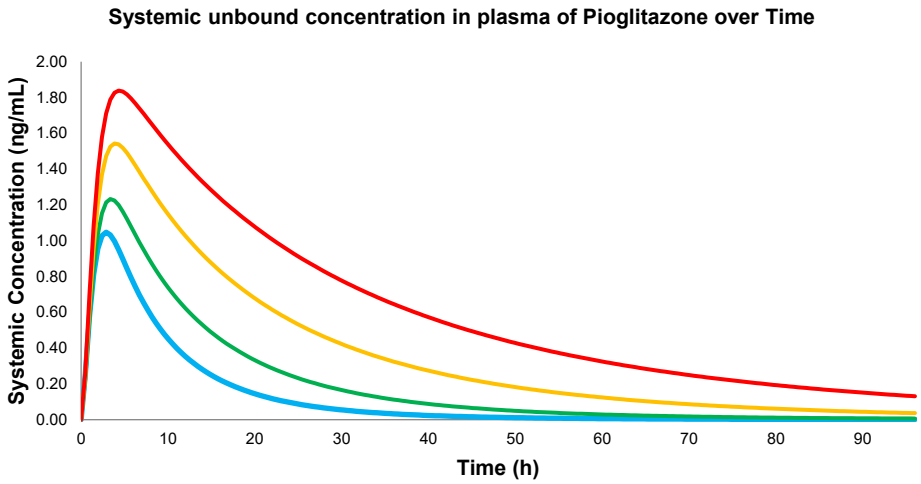

Figure 19. The unbound concentration–time curve of pioglitazone in virtual populations.

The blue solid line represents the healthy population; green represents Child-Pugh A; yellow Child-Pugh B; and red Child-Pugh C.

Table 14. PK parameters of unbound pioglitazone in virtual populations

PK parameters	Healthy	Child-Pugh A	GMR	Child-Pugh B	GMR	Child-Pugh C	GMR
C_{max} (ng/mL)	2.021	2.298	1.14	2.679	1.33	3.151	1.57
AUC_{last} (h·ng/mL)	10.168	17.819	1.78	27.615	2.82	42.733	4.56
T_{max} (h)	0.721	0.720		0.961		0.961	

Abbreviations: C_{max}, peak concentration; AUC_{last}, area under concentration-time curve at the last quantifiable time; T_{max}, time to C_{max}; GMR, geometric mean ratio; All data shown as mean values with standard deviation.

연세대학교
YONSEI UNIVERSITY

3.3.2. Hepatic Clearance of TZDs in Patients with Hepatic Impairment

The total hepatic intrinsic clearance of the TZDs showed a significant decrease with increasing severity of hepatic impairment (Table 15). There were dynamic changes in enzymatic clearance in the metabolism of each TZD. CYP3A4 predominantly contributed to the metabolism of lobeglitazone in the healthy population. The contribution of CYP3A4 to the metabolism of lobeglitazone decreased with increasing severity of hepatic impairment. In contrast, the contribution of CYP2C8, the main metabolizing enzyme for rosiglitazone and pioglitazone, remained the same regardless of disease severity.

연세대학교
YONSEI UNIVERSITY

Table 15. Comparison of intrinsic clearance and contribution of hepatic enzymes in different virtual populations.

	Lobeglitazone						
	Healthy population	Child-Pugh A	GMR	Child-Pugh B	GMR	Child-Pugh C	GMR
CL_{int} (L/h)	2144	1322	0.62	752	0.35	496	0.23
Contribution of CYPs (%)							
CYP3A4	34	35		25		17	
CYP2D6	18	17		10		4	
CYP2C19	14	6		6		4	
Additional HLM	34	42		59		75	
	Rosiglitazone						
CL_{int} (L/h)	1065	611	0.57	386	0.36	235	0.22
Contribution of CYPs (%)							
CYP2C8	56	51		48		43	
CYP2C9	31	30		28		24	
Additional HLM	13	19		24		33	
	Pioglitazone						

연세대학교
YONSEI UNIVERSITY

CL_{int} (L/h)	357	209	0.58	115	0.32	64	0.18
Contribution of CYPs (%)							
CYP2C8	57	48		54		52	
CYP3A4	37	43		32		27	
Additional HLM	6	9		14		21	

Abbreviation: CL_{int}, intrinsic clearance; CYP, cytochrome P; HLM, human liver microsomes; GMR, geometric mean ratio. Data shown in mean values.

연세대학교
YONSEI UNIVERSITY

4. Discussion

In this study, PBPK models of three TZDs were successfully developed and validated in healthy subjects, and the simulation of PK parameters was performed in patients with hepatic impairment according to the Child-Pugh classification system.

The simulation results of the lobeglitazone PBPK model tended to slightly overpredict the exposure in patients with hepatic impairment when compared to the observed value in Child-Pugh A and B patients. However, the PE of the current model was insignificant and was within the acceptable range of evaluation. The simulation of the rosiglitazone PBPK model in this study was consistent with the clinical observations in Child-Pugh B and C patients, showing decreased C_{max} and increased AUCs in these patients (Miller et al. 1999). The simulation with the current PBPK model for pioglitazone tended to overpredict the exposure compared to the observations in Child-Pugh B or C patients (Eckland, Danhof 2000). The low prediction capability of the pioglitazone model might be due to the following reasons: this model was adopted the transporter activities in terms of activity hepatic scalar, which would be gradually decreased by the severity of hepatic impairment. However, the actual transporter expressions and functions could be both elevated and decreased in various hepatic disease states (Thakkar, Slizgi, Brouwer 2017). The intraindividual variability of the main metabolic enzyme CYP2C8*3 (appeared 2-fold compared to wild-type for Caucasians) was not considered in the clinical trial

연세대학교
YONSEI UNIVERSITY

used for the validation of the model (Kirchheiner et al. 2005). In addition, the PBPK modeling methods would naturally overpredict the exposure of drugs in hepatic impairment, especially for CYP3A4 substrates (Heimbach et al. 2021, Johnson et al. 2010).

Compared to previous studies, this study tried to apply a full-body distribution model to develop PBPK models for TZDs. Several studies had developed PBPK models of rosiglitazone and pioglitazone by adopting the minimal compartment model of distribution, which considers the liver as the only separate compartment and lumping the rest of the organs (Hruska et al. 2005, Tan et al. 2019, Yeo-Rowland, Kenny, Rostami-Hodjegan 2013). The minimal compartment model of distribution could be very useful to predict drug interaction studies or genetic polymorphisms but not to be applicable to predict PK parameters in patients with hepatic insufficiency. The current PBPK models of the TZDs were able to adopt the changes of as many as available factors in hepatic impairment such as functional liver volumes, different hepatic enzyme activities, related blood flow, and serum proteins according to the Child-Pugh classification system. Therefore, the simulation results of this study might have significance in predicting PK parameters in patients with hepatic insufficiency without conducting clinical trials for the patients of each Child-Pugh class. However, there would be several limitations to be improved in the future studies. Because lobeglitazone was approved and marketed only in Korea, all clinical trials were conducted in Korean subjects. However, the virtual population of hepatic

연세대학교
YONSEI UNIVERSITY

impairment on the SimCYP^{TM} platform was constructed based on Caucasian patients (Johnson 2010). Thus, it would be necessary to construct a population database suitable for Korean patients with hepatic impairment and conduct further research in the relevant populations.

The simulation results of the current models could be also useful to give additional information under conditions when it would not be feasible to observe changes in clinical trials. For example, the unbound fractions of lobeglitazone and pioglitazone could not be analyzed due to the nature of ultra-highly binding to proteins in clinical trials with the methods confirmed from *in vitro* experiments. Usually, the increase in unbound fraction in the patients with hepatic impairment would be associated with unexpected pharmacological effects (Verbeeck 2008, Schmidt, Gonzalez, Derendorf 2009).

The simulation results of these PBPK models for TZDs in patients with hepatic impairment by the severity referred to Child-Pugh classification system showed the following characteristics. In the Child-Pugh A patients, the GMRs of C_{max} and AUCs were close to those in healthy subjects for all TZDs. Although the exposure of the unbound fractions in Child-Pugh A patients showed a slight increase, the changes were not significant. For lobeglitazone and rosiglitazone, the GMRs of the AUCs were less than 2.0 in the Child-Pugh B patients. However, the calculated results based on these PBPK models showed that the unbound fraction exposure of

연세대학교
YONSEI UNIVERSITY

rosiglitazone increased by more than 3-fold in Child-Pugh B patients. For pioglitazone, the AUCs of unbound fractions in both Child-Pugh B and C patients increased by more than 2-fold, and the unbound fraction exposure of pioglitazone significantly increased by 3- and 4-fold, respectively.

Regulatory organizations have recommended that if the GMR of AUCs is greater than 2.0 compared to that in healthy subjects at the recommended dose, the dose adjustment must be stated clearly on the label (Verbeeck 2008). The significantly increased unbound fraction in patients with hepatic impairment by the severity could also cause unexpected pharmacological effects. The simulation results of this study could provide PK parameters that would not be obtained from clinical trials. Hence, PBPK modeling and simulation might be useful as references to supplement clinical trial data when treating patients with hepatic impairment.

연세대학교
YONSEI UNIVERSITY

5. Conclusion

In this study, PBPK models of the marketed TZDs (lobeglitazone, rosiglitazone, and pioglitazone) were developed to predict PK parameters. The predicted concentration–time curves and PK parameters of the developed PBPK models were consistent with observed clinical trial data in the healthy population. The simulation results of the validated models could provide useful information in patients with hepatic impairment. This study illustrates that PBPK modeling and simulation would be a useful tool to predict PK alterations in patients with hepatic impairment classified according to the Child-Pugh system under conditions when clinical trials cannot be conducted in those patients.

연세대학교
YONSEI UNIVERSITY

References

Bae J, Park T, Kim H, Lee M, Cha BS. "Lobeglitazone: A Novel Thiazolidinedione for the Management of Type 2 Diabetes Mellitus." *Diabetes Metab J* 45, no. 3 (2021): 326-36. doi:10.4093/dmj.2020.0272.

Baldwin SJ, Clarke SE, Chenery RJ. "Characterization of the cytochrome P450 enzymes involved in the in vitro metabolism of rosiglitazone." *Br J Clin Pharmacol* 48, no. 3 (1999): 424-32. doi:10.1046/j.1365-2125.1999.00030.x.

Bazargan M, Foster DJ, Davey AK, Muhlhausler BS. "Rosiglitazone Metabolism in Human Liver Microsomes Using a Substrate Depletion Method." *Drugs R D* 17, no. 1 (2017): 189-98. doi:10.1007/s40268-016-0166-4.

Bowman CM, Benet LZ. "In vitro-in vivo extrapolation and hepatic clearance-dependent underprediction." *J Pharm Sci* 108, no. 7 (2019): 2500-4.

Cariou B, Charbonnel B, Staels B. "Thiazolidinediones and PPARγ agonists: time for a reassessment." *Trends Endocrinol Metab* 23, no. 5 (2012): 205-15. doi:https://doi.org/10.1016/j.tem.2012.03.001.

Chang C, Pang KS, Swaan PW, Ekins S. "Comparative pharmacophore modeling of organic anion transporting polypeptides: a meta-analysis of rat Oatp1a1 and human OATP1B1." *J Pharmacol Exp Ther* 314, no. 2 (2005): 533-41. doi:10.1124/jpet.104.082370.

연세대학교
YONSEI UNIVERSITY

Chiba M, Ishii Y, Sugiyama Y. "Prediction of hepatic clearance in human from in vitro data for successful drug development." *AAPS J* 11, no. 2 (2009): 262-76. doi:10.1208/s12248-009-9103-6.

Clark DE. "Rapid calculation of polar molecular surface area and its application to the prediction of transport phenomena. 2. Prediction of blood-brain barrier penetration." *J Pharm Sci* 88, no. 8 (1999): 815-21. doi:10.1021/js980402t.

Cox PJ, Ryan DA, Hollis FJ, Harris AM, Miller AK, Vousden M, Cowley H. "Absorption, disposition, and metabolism of rosiglitazone, a potent thiazolidinedione insulin sensitizer, in humans." *Drug Metab Dispos* 28, no. 7 (2000): 772-80.

Delcò F, Tchambaz L, Schlienger R, Drewe J, Krähenbühl S. "Dose adjustment in patients with liver disease." *Drug Saf* 28, no. 6 (2005): 529-45. doi:10.2165/00002018-200528060-00005.

Di L, Whitney-Pickett C, Umland JP, Zhang H, Zhang X, Gebhard DF, Lai Y, Federico JJ, Davidson RE, Smith R, Reyner EL, Lee C, Feng B, Rotter C, Varma MV, Kempshall S, Fenner K, El-kattan AF, Liston TE, Troutman MD. "Development of a new permeability assay using low-efflux MDCKII cells." *J Pharm Sci* 100, no. 11 (2011): 4974-85. doi:https://doi.org/10.1002/jps.22674.

연세대학교
YONSEI UNIVERSITY

Eckland D, Danhof M. "Clinical pharmacokinetics of pioglitazone." *Exp Clin Endocrinol Diabetes* 108, no. Sup. 2 (2000): 234-42. doi:10.1055/s-2000-8525.

El-Khateeb E, Burkhill S, Murby S, Amirat H, Rostami-Hodjegan A, Ahmad A. "Physiological-based pharmacokinetic modeling trends in pharmaceutical drug development over the last 20-years; in-depth analysis of applications, organizations, and platforms." *Biopharm Drug Dispos* 42, no. 4 (2021): 107-17. doi:10.1002/bdd.2257.

Hanefeld M. "Pharmacokinetics and clinical efficacy of pioglitazone." *Int J Clin Pract Suppl*, no. 121 (2001): 19-25.

Heimbach T, Chen Y, Chen J, Dixit V, Parrott N, Peters SA, Poggesi I, Sharma P, Snoeys J, Shebley M, Tai G, Tse S, Upreti VV, Wang YH, Tsai A, Xia B, Zheng M, Zhu AZX, Hall S. "Physiologically-Based Pharmacokinetic Modeling in Renal and Hepatic Impairment Populations: A Pharmaceutical Industry Perspective." *Clin Pharmacol Ther* 110, no. 2 (2021): 297-310. doi:https://doi.org/10.1002/cpt.2125.

Hruska MW, Amico JA, Langaee TY, Ferrell RE, Fitzgerald SM, Frye RF. "The effect of trimethoprim on CYP2C8 mediated rosiglitazone metabolism in human liver microsomes and healthy subjects." *Br J Clin Pharmacol* 59, no. 1 (2005): 70-9. doi:https://doi.org/10.1111/j.1365-2125.2005.02263.x.

연세대학교
YONSEI UNIVERSITY

Jaakkola T, Laitila J, Neuvonen PJ, Backman JT. "Pioglitazone is metabolised by CYP2C8 and CYP3A4 in vitro: potential for interactions with CYP2C8 inhibitors." *Basic Clin Pharmacol Toxicol* 99, no. 1 (2006): 44-51. doi:10.1111/j.1742-7843.2006.pto_437.x.

Jaakkola T, Backman JT, Neuvonen M, Neuvonen PJ. "Effects of Gemfibrozil, Itraconazole, and Their Combination on the Pharmacokinetics of Pioglitazone." *Clin Pharmacol Ther* 77, no. 5 (2005): 404-14. doi:https://doi.org/10.1016/j.clpt.2004.12.266.

Jamei M, Marciniak S, Feng K, Barnett A, Tucker G, Rostami-Hodjegan A. "The Simcyp® Population-based ADME Simulator." *Exp Opin Drug Metab Toxicol* 5, no. 2 (2009): 211-23. doi:10.1517/17425250802691074.

Johnson TN, Boussery K, Rowland-Yeo K, Tucker GT, Rostami-Hodjegan A. "A semi-mechanistic model to predict the effects of liver cirrhosis on drug clearance." *Clin Pharmacokinet* 49, no. 3 (2010): 189-206. doi:10.2165/11318160-000000000-00000.

Jónsdóttir SO, Jørgensen FS, Brunak S. " Prediction methods and databases within chemoinformatics: emphasis on drugs and drug candidates." *Bioinformatics* 21, no.10 (2005): 2145-2160. doi:10.1093/bioinformatics/bti314.

Kazmi F, Hensley T, Pope C, Funk RS, Loewen GJ, Buckley DB, Parkinson A. "Lysosomal sequestration (trapping) of lipophilic amine (cationic amphiphilic) drugs in immortalized human hepatocytes (Fa2N-4 cells)."

연세대학교
YONSEI UNIVERSITY

Drug Metab Dispos 41, no. 4 (2013): 897-905. doi:10.1124/dmd.112.050054.

Kim JW, Kim JR, Yi S, Shin KH, Shin HS, Yoon SH, Cho JY, Kim DH, Shin SG, Jang IJ, Yu KS. "Tolerability and pharmacokinetics of lobeglitazone (CKD-501), a peroxisome proliferator-activated receptor-γ agonist: a single- and multiple-dose, double-blind, randomized control study in healthy male Korean subjects." *Clin Ther* 33, no. 11 (2011): 1819-30. doi:10.1016/j.clinthera.2011.09.023.

Kirchheiner J, Roots I, Goldammer M, Rosenkranz B, Brockmöller J. "Effect of genetic polymorphisms in cytochrome p450 (CYP) 2C9 and CYP2C8 on the pharmacokinetics of oral antidiabetic drugs: clinical relevance." *Clin Pharmacokinet* 44, no. 12 (2005): 1209-25. doi:10.2165/00003088-200544120-00002.

Lee JH, Noh CK, Yim CS, Jeong YS, Ahn SH, Lee W, Kim DD, Chung SJ. "Kinetics of the Absorption, Distribution, Metabolism, and Excretion of Lobeglitazone, a Novel Activator of Peroxisome Proliferator-Activated Receptor Gamma in Rats." *J Pharm Sci* 104, no. 9 (2015): 3049-59. doi:10.1002/jps.24378.

Lennernäs H. "Regional intestinal drug permeation: biopharmaceutics and drug development." *Eur J Pharm Sci* 57 (2014): 333-41. doi:10.1016/j.ejps.2013.08.025.

연세대학교
YONSEI UNIVERSITY

Malinowski JM, Bolesta S. "Rosiglitazone in the treatment of type 2 diabetes mellitus: a critical review." *Clin Ther* 22, no. 10 (2000): 1151-68; discussion 49-50. doi:10.1016/s0149-2918(00)83060-x.

Mathew S, Tess D, Burchett W, Chang G, Woody N, Keefer C, Orozco C, Lin J, Jordan S, Yamazaki S, Jones R, Di L. "Evaluation of Prediction Accuracy for Volume of Distribution in Rat and Human Using In Vitro, In Vivo, PBPK and QSAR Methods." *J Pharm Sci* 110, no. 4 (2021): 1799-823. doi:10.1016/j.xphs.2020.12.005.

Matsumoto Y, Cabalu T, Sandhu P, Hartmann G, Iwasa T, Yoshitsugu H, Gibson C, Uemura N. "Application of Physiologically Based Pharmacokinetic Modeling to Predict Pharmacokinetics in Healthy Japanese Subjects." *Clin Pharmacol Ther* 105, no. 4 (2019): 1018-30. doi:https://doi.org/10.1002/cpt.1240.

Miller AK, Inglis AL, Thompson K, Davie CC, Schenker S, Blum R, Jorkasky D, Freed MI, Beecham SK. "Effect of Hepatic Impairment on The Pharmacokinetics (PK) of Rosiglitazone (RSG)." *Clin Pharmacol Ther* 65, no. 2 (1999): 186-. doi:https://doi.org/10.1016/S0009-9236(99)80274-4.

Ogurtsova K, da RochaFernandes JD, Huang Y, Linnenkamp U, Guariguata L, Cho NH, Cavan D, Shaw JE, Makaroff LE. "IDF Diabetes Atlas: Global estimates for the prevalence of diabetes for 2015 and 2040." *Diabetes Res Clin Pract* 128 (2017): 40-50. doi:10.1016/j.diabres.2017.03.024.

연세대학교
YONSEI UNIVERSITY

Park J. "Effect of rifampin on the pharmacokinetics of rosiglitazone in healthy subjects." *Clin Pharmacol Ther* 75, no. 3 (2004): 157-62. doi:10.1016/j.clpt.2003.10.003.

Park MK, Kim TE, Kim J, Kim C, Yoon SH, Cho JY, Jang IJ, Yu KS, Lim KS. "Tolerability and pharmacokinetics of lobeglitazone, a novel peroxisome proliferator-activated receptor-γ agonist, after a single oral administration in healthy female subjects." *Clin Drug Investig* 34, no. 7 (2014): 467-74. doi:10.1007/s40261-014-0197-y.

Pathak SM, Ruff A, Kostewicz ES, Patel N, Turner DB, Jamei M. "Model-Based Analysis of Biopharmaceutic Experiments To Improve Mechanistic Oral Absorption Modeling: An Integrated in Vitro in Vivo Extrapolation Perspective Using Ketoconazole as a Model Drug." *Mol Pharm* 14, no. 12 (2017): 4305-20. doi:10.1021/acs.molpharmaceut.7b00406.

Picardi A, D'Avola D, Gentilucci UV, Galati G, Fiori E, Spataro S, Afeltra A. "Diabetes in chronic liver disease: from old concepts to new evidence." *Diabetes Metab Res Rev* 22, no. 4 (2006): 274-83. doi:10.1002/dmrr.636.

Poulin P, Theil FP. "Prediction of pharmacokinetics prior to in vivo studies. 1. Mechanism-based prediction of volume of distribution." *J Pharm Sci* 91, no. 1 (2002): 129-56. doi:10.1002/jps.10005.

연세대학교
YONSEI UNIVERSITY

Proctor NJ, Tucker GT, Rostami-Hodjegan A. "Predicting drug clearance from recombinantly expressed CYPs: intersystem extrapolation factors." *Xenobiotica* 34, no. 2 (2004): 151-78. doi:10.1080/00498250310001646353.

Rodgers T, Leahy D, Rowland M. "Physiologically based pharmacokinetic modeling 1: predicting the tissue distribution of moderate-to-strong bases." *J Pharm Sci* 94, no. 6 (2005a): 1259-76. doi:10.1002/jps.20322.

Rodgers T, Leahy D, Rowland M. "Tissue distribution of basic drugs: accounting for enantiomeric, compound and regional differences amongst beta-blocking drugs in rat." *J Pharm Sci* 94, no. 6 (2005b): 1237-48. doi:10.1002/jps.20323.

Rodgers T, Rowland M. "Mechanistic approaches to volume of distribution predictions: understanding the processes." *Pharm Res* 24, no. 5 (2007): 918-33. doi:10.1007/s11095-006-9210-3.

Rodighiero V. "Effects of liver disease on pharmacokinetics. An update." *Clin Pharmacokinet* 37, no. 5 (1999): 399-431. doi:10.2165/00003088-199937050-00004.

Rostami-Hodjegan A, Tucker GT. "Simulation and prediction of in vivo drug metabolism in human populations from in vitro data." *Nat Rev Drug Discov* 6, no. 2 (2007): 140-8. doi:10.1038/nrd2173.

Schmidt S, Gonzalez D, Derendorf H. "Significance of Protein Binding in Pharmacokinetics and Pharmacodynamics. " *J Pharm Sci* 99 no. 3 (2010): 1107-1122. doi:10.1002/jps.21916.

연세대학교
YONSEI UNIVERSITY

Schmitt MV, Reichel A, Liu X, Fricker G, Lienau P. "Extension of the Mechanistic Tissue Distribution Model of Rodgers and Rowland by Systematic Incorporation of Lysosomal Trapping: Impact on Unbound Partition Coefficient and Volume of Distribution Predictions in the Rat." *Drug Metabolism and Disposition* 49, no. 1 (2021): 53-61. doi:10.1124/dmd.120.000161.

Soccio RE, Chen ER, Lazar MA. "Thiazolidinediones and the Promise of Insulin Sensitization in Type 2 Diabetes." *Cell Metab* 20, no. 4 (2014): 573-91. doi:https://doi.org/10.1016/j.cmet.2014.08.005.

Tan ML, Zhao P, Zhang L, Ho YF, Varma MVS, Neuhoff S, Nolin TD, Galetin A, Huang SM. "Use of Physiologically Based Pharmacokinetic Modeling to Evaluate the Effect of Chronic Kidney Disease on the Disposition of Hepatic CYP2C8 and OATP1B Drug Substrates." *Clin Pharmacol Ther* 105, no. 3 (2019): 719-29. doi:https://doi.org/10.1002/cpt.1205.

Thakkar N, Slizgi JR, Brouwer KLR. "Effect of Liver Disease on Hepatic Transporter Expression and Function." *J Pharm Sci* 106, no. 9 (2017): 2282-94. doi:10.1016/j.xphs.2017.04.053.

Tolman KG, Fonseca V, Dalpiaz A, Tan MH. "Spectrum of liver disease in type 2 diabetes and management of patients with diabetes and liver disease." *Diabetes Care* 30, no. 3 (2007): 734-43. doi:10.2337/dc06-1539.

연세대학교
YONSEI UNIVERSITY

Türk D, Hanke N, Lehr T. "A Physiologically-Based Pharmacokinetic Model of Trimethoprim for MATE1, OCT1, OCT2, and CYP2C8 Drug–Drug–Gene Interaction Predictions." *Pharmaceutics* 12, no. 11 (2020): 1074.

Tylutki Z, Polak S, Wiśniowska B. "Top-down, Bottom-up and Middle-out Strategies for Drug Cardiac Safety Assessment via Modeling and Simulations." *Curr Pharmacol Rep* 2, no. 4 (2016): 171-7. doi:10.1007/s40495-016-0060-3.

Uchimura T, Kato M, Saito T, Kinoshita H. "Prediction of human blood-to-plasma drug concentration ratio." *Biopharm Drug Dispos* 31, no. 5-6 (2010): 286-97. doi:10.1002/bdd.711.

Varma MV, Gardner I, Steyn SJ, Nkansah P, Rotter CJ, Whitney-Pickett C, Zhang H, Di L, Cram M, Fenner KS, El-Kattan AF. "pH-Dependent solubility and permeability criteria for provisional biopharmaceutics classification (BCS and BDDCS) in early drug discovery." *Mol Pharm* 9, no. 5 (2012): 1199-212. doi:10.1021/mp2004912.

Verbeeck RK. "Pharmacokinetics and dosage adjustment in patients with hepatic dysfunction." *Eur J Clin Pharmacol* 64, no. 12 (2008): 1147-61. doi:10.1007/s00228-008-0553-z.

Winiwarter S, Bonham NM, Ax F, Hallberg A, Lennernäs H, Karlén A. "Correlation of human jejunal permeability (in vivo) of drugs with experimentally and

연세대학교
YONSEI UNIVERSITY

theoretically derived parameters. A multivariate data analysis approach." *J Med Chem* 41, no. 25 (1998): 4939-49. doi:10.1021/jm9810102.

Wishart DS, Feunang YD, Guo AC, Lo EJ, Marcu A, Grant JR, Sajed T, Johnso D, Li C, Sayeeda Z, Assempour N, Iynkkaran I, Liu Y, Maciejewski A, Gale N, Wilson A, Chin L, Cummings R, Le D, Pon A, Knox C, Wilson M. "DrugBank 5.0: a major update to the DrugBank database for 2018." *Nucleic Acids Res* 46, no. D1 (2018): D1074-d82. doi:10.1093/nar/gkx1037.

Xiao Q, Tang L, Xu R, Qian W, Yang J. "Physiologically based pharmacokinetics model predicts the lack of inhibition by repaglinide on the metabolism of pioglitazone." *Biopharm Drug Dispos* 36, no. 9 (2015): 603-12. doi:10.1002/bdd.1987.

Rowland-Yeo K, Kenny JR, Rostami-Hodjegan A. "Application of in vitro–in vivo extrapolation (IVIVE) and physiologically based pharmacokinetic (PBPK) modelling to investigate the impact of the CYP2C8 polymorphism on rosiglitazone exposure." *Eur J Clin Pharmacol* 69, no. 6 (2013): 1311-20. doi:10.1007/s00228-012-1467-3.

Yim CS, Jeong YS, Lee SY, Pyeon W, Ryu HM, Lee JH, Lee KR, Maeng HJ, Chung SJ. "Specific Inhibition of the Distribution of Lobeglitazone to the Liver by Atorvastatin in Rats: Evidence for a Rat Organic Anion Transporting Polypeptide 1B2–Mediated Interaction in Hepatic Transport." *Drug Metab Dispos* 45, no. 3 (2017): 246. doi:10.1124/dmd.116.074120.

연세대학교
YONSEI UNIVERSITY

Zhao P, Zhang L, Grillo JA, Liu Q, Bullock JM, Moon YJ, Song P, Brar SS, Madabushi R, Wu TC, Booth BP, Rahman NA, Reynolds KS, Gil BE, Lesko LJ, Huang SM. "Applications of physiologically based pharmacokinetic (PBPK) modeling and simulation during regulatory review." *Clin Pharmacol Ther* 89, no. 2 (2011): 259-67. doi:10.1038/clpt.2010.298.

Zhuang X, Lu C. "PBPK modeling and simulation in drug research and development." *Acta Pharm Sin B* 6, no. 5 (2016): 430-40. doi:https://doi.org/10.1016/j.apsb.2016.04.004.

연세대학교
YONSEI UNIVERSITY

Appendices

Appendix 1. List of Abbreviations

Abbreviations	Full Name
A	the surface area of the cell membrane
$A_{b,ss}$	the total quantity of drug in the body at steady state
ADAM model	The advanced dissolution, absorption, and metabolism model
ADME	absorption, distribution, metabolism, and elimination
AUC_{inf}	the area under concentration-time curve extrapolated to the infinite
AUC_{last}	the area under concentration-time curve at the last quantifiable time
B/P	the blood-to-plasma ratio
CACO-2	colorectal adenocarcinoma-2
C_{in}	the inlet drug concentration
C_{max}	peak concentration
C_{out}	the outlet drug concentration
$C_{p,ss}$	the total drug concentration in plasma at steady state
C_{pu}	the drug concentration of unbound fraction in plasma
C_{rbc}	the drug concentration in red blood cell
$C_{t,ss}$	the total drug concentration in a tissue at steady state
$D_{o:w}$	the distribution coefficient
E_g	Gut wall extraction ratio
E_h	Hepatic extraction ratio

연세대학교
YONSEI UNIVERSITY

Abbreviations	Full Name
ECF	extracellular fluid
f	the fractional tissue volume
f_a	the fraction of dose entering the cellular space of the enterocytes
F_g	gut availability (fraction of drug escaping gut metabolism). i.e., fraction of the absorbed dose that is not metabolized in the gut wall
F_H	hepatic availability (fraction of drug escaping hepatic metabolism)
F_{oral}	bioavailability
f_u	unbound fraction
GI tract	gastrointestinal tract
HBD	the number of hydrogen bond donors
HLM	the additional clearance of human liver microsomes
Ht_{human}	hematocrit human
Ht_{human}	ratio of hematocrit in human
Ht_{rat}	ratio of Hematocrit in rat
ISEF	intersystem extrapolation factors
IVIVE	*in vitro–in vivo* extrapolation
ICF	intracellular fluid
J^{total}	the net flux of molecules across the cell membrane
$J^{unbound,ionized}$	the net flux of unbound and ionized molecules across the cell membrane
$J^{unbound,unionized}$	the net flux of unbound and unionized molecules across the cell membrane
k_a	a single first-order absorption rate constant
K_{ap}	the affinity constant of a drug for acidic phospholipid

연세대학교
YONSEI UNIVERSITY

Abbreviations	Full Name
$Kp_{uu,uu}$	the ratio of the unbound, unionised tissue concentration to the unbound, unionised plasma concentration
k_t	the small intestinal transit rate constant
l	the intestinal length
MMPGL	milligrams of microsomal proteins per gram of liver
OATPs	Organic anion transporting polypeptides
P	partition coefficient
P_{aff}	the apparent permeability coefficients
PE	prediction errors
P_{eff}	the effective gut wall permeability coefficients
$P_{o:w}$	the partition coefficient
PSA	polar surface area (Å)
$P_{t:p}$	the tissue-partition coefficient
Qin	the perfusion flow rate
R	the intestinal radius
rhCYP	recombinant human cytochrome P
T_{max}	time to peak concentration
TZD	thiazolidinediones
ub	unbound
ui	unionized
V_e	the volume of erythrocytes
V_{nlt}	the fractional volume of neutral lipids (nl) in tissue (t)
V_p	the volume of plasma

연세대학교
YONSEI UNIVERSITY

Abbreviations	Full Name
V_{plp}	the fractional volume of phospholipids (pl) in plasma (p)
V_{plt}	the fractional volume of phospholipids (pl) in tissue (t)
V_{ss}	the volume of distribution of a drug
V_t	the volume of tissue
V_{wp}	the fractional volume of water (w) in plasma (p)
V_{wt}	the fractional volume of water (w) in tissue (t)
$X_{observed}$	the observed geometric mean of major PK parameters
$X_{predicted}$	the simulated geometric mean of major PK parameters

연세대학교
YONSEI UNIVERSITY

Appendix 2. Visual Predictive Check with PBPK model of Lobeglitazone in Individual Subjects

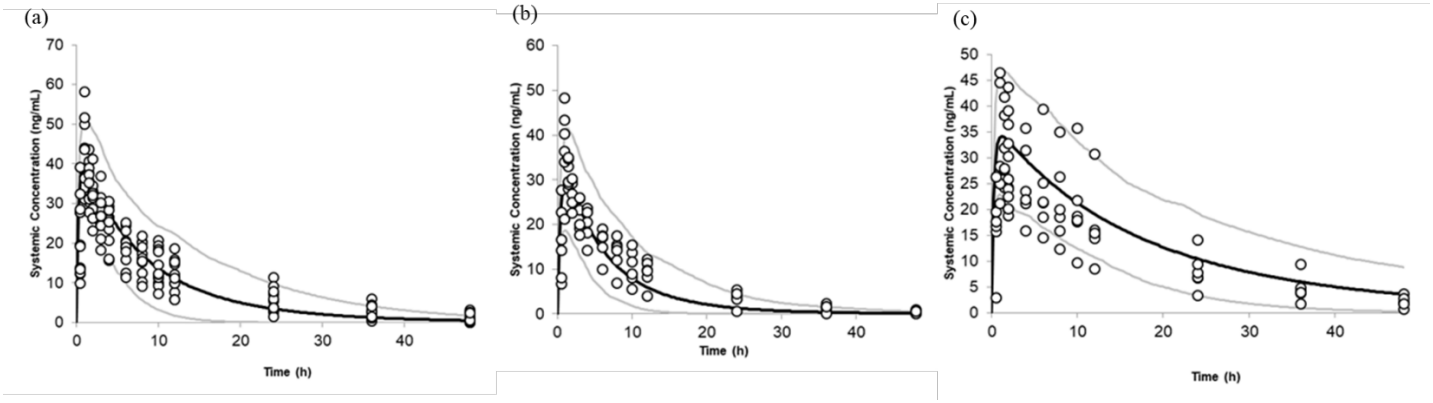

Appendix Figure 1. Visual predictive check for lobeglitazone PBPK models in (a) healthy subjects, (b) Child-Pugh A patients, (c) Child-Pugh B patients

Dots indicate the observed data. The solid line represents the mean value of the simulation. Grey lines are the lowest and the highest values within 95% confidence levels.

연세대학교
YONSEI UNIVERSITY

Abstract (Korean)

간기능 장애 환자에서 티아졸리디네이온계 약물의 생리학 기반 약동학 모델링과 시뮬레이션

연세대학교
일반대학원
제약의료규제과학 협동과정
박정신

I. 연구 배경

당뇨환자에서 간 질환의 유병율은 매우 높다. 간은 혈당 조절 및 약물의 대사를 담당하는 주요 장기이기 때문에 항당뇨제의 간 질환 환자에서 약동학적 평가는 필수적이다.

티아졸리딘디온은 과산화소체 증식제-활성화 수용체 감마 (Peroxisome proliferator-activated receptor gamma)의 작용제로 인슐린 민감성을 향상시켜

연세대학교
YONSEI UNIVERSITY

혈당을 조절한다. 현재 국내 시판되는 티아졸리딘디온 계열의 약물은 로베글리타존, 로지글리타존, 피오글리타존이 있다. 이들 약은 경구로 투여한 후 높은 생체이용율 (80~90%)를 보이고, 혈중 최고 농도가 약 1 시간 정도로 빨리 도달한다. 혈중 단백질 중 알부민과 결합력이 높고 (99% 이상 결합), 간에서 대사되어 소실되며 소변으로 배출되는 모체의 양은 거의 없으므로 약물의 소실 주요 소실 경로는 간 효소에 의한 대사이다. 따라서 간기능 장애 중증도에 따른 이들 약물의 약동학 매개 변수는 영향을 받을 것으로 예상되지만, 알려진 근거는 미미하다. 원칙적으로는 간질환 환자를 대상으로 한 임상시험을 수행하여 결과를 얻어야 하지만, 환자 모집의 어려움과 안전성 문제로 질환을 가진 환자 대상의 임상시험을 시도하는 데에는 많은 어려움이 있다. 그 해결책으로 최근 약동학 모델링과 시뮬레이션 방법이 각광받고 있다.

생리학 기반 약물동태 (Physiologically based Pharmacokinetics, PBPK) 모델링과 시뮬레이션 방법은 물질의 특성 및 생화학적 반응과 생리학적 특징들을 결합하여 투여된 약물의 흡수, 분포, 대사 및 소실을 예측할 수 있게 해 준다. 특히, 임상시험 수행이 특정 질환 환자나 소아, 임산부에서 약동학 매개변수를 예측하는데 유용하는데 활용될 수 있다.

연세대학교
YONSEI UNIVERSITY

본 연구에서는 로베글리타존, 로지글리타존, 피오글리타존의 PBPK 모델을 구축하여 타당성을 확인한 다음, Child-Pugh 분류에 따라 간기능 장애 중증도별로 환자에서 시뮬레이션 하여 약동학적 변화를 예측하였다.

II. 연구내용 및 방법

인구학 기반 소프트웨어인 SimCYP^{TM} (Certara, St. Louis, MO, USA)을 활용하여 로베글리타존, 로지글리타존, 피오글리타존의 PBPK 모델을 구축하였다. 사용된 약물의 물리화학적 특성은 공개된 데이터베이스인 DrugBank (go.drugbank.com)를 통해 얻었고, 필요한 시험관내 자료 및 Child-Pugh 분류에 따른 중증도별 간기능 장애 환자의 약동학에 영향을 미치는 생리학적 요인들을 반영하여 인구학적 정보를 완성하였다.

로베글리타존과 로지글리타존에 대한 PBPK 모델의 흡수는 일차 동적 흡수 모델을, 피오글리타존에 대한 PBPK 모델의 흡수는 Advanced dissolution, absorption, and metabolism (ADAM) 모델을 적용하였으며, 분포는 신체 주요 기관을 각 구획으로 나눈 전신 분포(Full-body distribution) 모델을 적용하였다. 약물 제거는 효소 반응 속도 모델 (enzyme kinetic elimination model)을 활용하였다.

연세대학교
YONSEI UNIVERSITY

만들어진 모델은 건강 성인 약동학 임상시험의 환자 인구학적 정보 중 연령 및 성별을 일치시켜 시뮬레이션 하였다. 그 결과를 비교하였을 때, 주요 약동학적 매개 변수(최고 혈중 농도 (the peak concentration, C_{max})) 및 약물농도-시간 곡선하 면적 (the area under the concentration-time curve, (AUC))의 예측값과 관찰값의 비가 0.5-2.0 에 포함되는지 확인하여 타당성을 검증하였다. 로베글리타존의 경우, Child-Pugh A 와 B 에 해당하는 환자의 임상시험 결과와 비교하여 타당성을 추가적으로 검증하였다.

검증된 각 약물의 모델은 정상인과 각 중증도별 연령 범위 18-65 세, 남녀 성별을 50:50 으로 하여 100 명의 가상의 환자에서 간기능 장애 중증도에 따라 Child-Pugh 분류로 구별하여 시뮬레이션한 후 주요 약동학적 매개 변수를 비교하였다.

III. 연구 결과

만들어진 로베글리타존, 로지글리타존, 피오글리타존의 PBPK 모델은 건강 성인의 임상시험 결과와 비교하였을 때, 예측값과 관찰값의 비가 모두 타당한 범위에 들었다. 로베글리타존의 모델은 추가적으로 간기능 장애 환자에 적용하여 시뮬레이션 한 결과, 임상시험의 자료와 비교하였을 때 예측능력이 적절한 것을 확인하였다.

연세대학교
YONSEI UNIVERSITY

각 Child-Pugh 분류에 해당하는 가상의 간기능 장애 환자 100 명을 대상으로 시뮬레이션 하여 중증도에 따라 약동학 매개 변수를 비교한 결과, 티아졸리딘디온 계열 약물의 주요 약동학 매개 변수는 Child-Pugh A 환자군에서는 건강 성인과 비교하여 모두 유사하게 나타났다. 로베글리타존의 경우, Child-Pugh B 환자에서 AUC 와 C_{max} 의 기하평균 비는 각각 1.36 과 0.97 이었다. 로지글리타존은 Child-Pugh B 환자에서 AUC 와 C_{max} 의 기하평균 비가 각각 1.93 과 0.92 였다. 피오글리타존은 Child-Pugh B 환자에서 AUC 와 C_{max} 의 기하평균 비가 각각 2.19 와 1.03 이었다. 또 Child-Pugh C 환자에서 AUC 와 C_{max} 의 기하평균 비는, 로베글리타존은 각각 2.19 와 1.03, 로지글리타존은 2.26 와 0.81, 피오글리타존은 2.76 과 0.91 이었다. 추가적으로 분석한 결과에서 각 약물의 단백질 비결합 분율 (unbound fraction, f_u)의 변화가 유의미하게 나타났다. 건강 대상자와 비교하여 Child-Pugh A, B, C 에 해당하는 간기능 장애 환자에서 로베글리타존의 f_u 의 AUC 기하평균 비는 각각 1.51, 2.50, 3.62 였고, 로지글리타존은 각각 1.73, 3.23, 5.66, 피오글리타존은 각각 1.78, 2.82, 4,56 이었다.

IV. 고찰

본 연구에서는 티오졸리딘디온계 약물의 PBPK 모델에 대해 전신 분포 모델을 적용하여 Child-Pugh 분류를 반영한 간기능 장애 중증도에 따른 기능성

연세대학교
YONSEI UNIVERSITY

간 크기, 간효소의 활성도, 혈류량 변화, 혈청 단백질을 변화를 반영하여 약동학 매개 변수를 예측하는데 적합하도록 만들어졌다.

본 연구에서 시행된 티아졸리딘디온계 약물의 PBPK 모델링과 시뮬레이션은 각 Child-Pugh A, B, C 환자의 약동학적 매개변수를 가지고 용량 적절성을, f_u의 변화를 바탕으로 독성 여부를 평가하는데 적용될 수 있다. 본 연구에서 살펴본 세 가지의 티아졸리딘온계 약물은 Child-Pugh A 환자에서 용량 조절이나 안전성에 문제없이 사용할 수 있을 것으로 여겨진다. 로베글리타존의 경우 Child-Pugh B 환자에서 용량 조절 및 안전성에 대한 문제없이 사용할 수 있다. 로지글리타존은 Child-Pugh B 환자에서 용량 적절성은 고려하지 않아도 되나, 안전성에 대한 충분한 고려가 필요하다. 피오글리타존은 Child-Pugh B 환자에서 용량 및 안전성에 대한 충분한 고려가 필요하다. 이들 티아졸리딘디온의 약물은 Child-Pugh C 환자에서 약물 노출이 급격이 증가하고 독성도 야기될 수 있어 사용을 권장하지 않을 수 있다.

V. 결론

본 연구 결과, 생리학 기반 약물동태 모델링과 시뮬레이션 방법은 간기능 환자에서 중증도에 따라 용량 조절의 여부나 독성을 평가하는데 유용하게

연세대학교
YONSEI UNIVERSITY

사용할 수 있다. 따라서 본 연구의 모델링과 시뮬레이션 방법은 이들 환자군에서 임상시험의 수행이 어려운 조건하에서 추가적 정보를 제공할 수 있다.

핵심되는 말: 로베글리타존, 로지글리타존, 피오글리타존, 간기능 장애, 생리학 기반 약물동태학